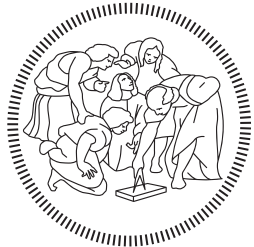


POLITECNICO DI MILANO  
Facoltà di Ingegneria  
Scuola di Ingegneria Industriale e dell'Informazione  
Dipartimento di Elettronica, Informazione e Bioingegneria  
Master of Science in Electronics Engineering



## Design and Implementation of a Driver for In-Wheel Brushless Motors for Unmanned Vehicles

Supervisor:

PROF. GIAMBATTISTA GRUOSSO

Co-Supervisor:

PROF. LUCA BASCETTA

Examiner:

PROF. LUIGI PIEGARI

Master Graduation Thesis by:

ARTURO MONTÚFAR ARREOLA  
Student Id n. 840541

Academic Year 2016-2017

## COLOPHON

This document was typeset using the typographical look-and-feel `classicthesis` developed by André Miede. The style was inspired by Robert Bringhurst's seminal book on typography "*The Elements of Typographic Style*". `classicthesis` is available for both L<sup>A</sup>T<sub>E</sub>X and LyX:

<http://code.google.com/p/classicthesis/>

The template has been adapted by Emanuele Mason, Andrea Cominola and Daniela Anghileri: *A template for master thesis at DEIB*, June 2015

*Final Version as of November 28, 2017 (classicthesis).*

To my family and friends:  
Thanks for supporting me while I'm learning to fly  
— Arturo



## ACKNOWLEDGMENTS

---

I want to thank the following people for helping me with the development of this work:

To Professor Giambattista Gruosso, for giving me the opportunity to develop such an interesting thesis project and for his guidance through the research method for this kind of projects, which is as valuable as the knowledge I gained regarding the topic developed in this work.

To Professor Luca Bascetta, for giving me advice and material regarding the research and implementation of the motor control theory and the work already developed regarding this project.

To Professor Luigi Piegari, for his support and advice on the final tests and the examination of the thesis.

To Professor Federico Terraneo, for his support and interest on the implementation of Miosix in this project, and to the Skyward Experimental Rocketry team, for their help with the CAN bus driver.

To Marco Bauer, for his support in the aspects related to the mechanics of the project and also for providing me with information of the work already developed.

To Giulio Fontana, for his support and advice regarding the manufacture of the systems developed for this work while working in the AIRLab.

To Professor Luigi Colombo for providing me documentation regarding the thermal management proposal developed in this work.

To Stefano Bianchi for helping with the fine details of the tuning of the controllers and with the development of the tests.

To Milica Jovanovic for helping me with the documentation of the software architecture and with the flowcharts.



## CONTENTS

---

Abstract	xiii
Estratto	xv
Preface	xvii
1 INTRODUCTION	1
2 PROBLEM STATEMENT	5
2.1 Technological Trade-Offs	5
2.2 Learning Curve	6
2.3 Motor Driver Development	6
2.4 Implementation of Field Oriented Control	6
3 MOTOR CONTROL THEORY	9
3.1 Electric Motor	9
3.1.1 Physical Principles	9
3.2 PMAC Motors	17
3.2.1 BLDC Motors	19
3.2.2 PMSM Motors	19
3.3 Electric Drives	20
3.3.1 Inverter	20
3.3.2 Angular Position Sensors	23
3.3.3 Current Sensors	25
3.3.4 Controller	26
3.4 PMAC Motors Driving Methods	27
3.4.1 Trapezoidal Drive	27
3.4.2 Sinusoidal Drive	32
3.5 Electric Motor Control Methods	33
3.5.1 Speed Control	34
3.5.2 Torque Control	35
3.5.3 Field Oriented Control	35
3.5.4 Speed Control with Field Oriented Control	37
4 STUDY CASE	39
4.1 Robi	39
4.2 In-Wheel Motors	40
4.3 Power Architecture	41
4.4 Electronic Architecture	41
5 PROJECT DEVELOPMENT	43
5.1 Hypothesis	43
5.2 VESC Board	43
5.2.1 Power Supply Input	44
5.2.2 Power MOSFET Three-Phase Inverter	48
5.2.3 MOSFET Driver	48
5.2.4 Microcontroller Unit	49
5.2.5 PCB Layout	50
5.3 Measurement Board	50

5.3.1	Voltage Measurement	50
5.3.2	Current Measurement	50
5.3.3	Data acquisition	50
5.4	Angular Position Sensor	50
5.5	Miosix	50
5.6	Test Setup	51
5.6.1	Robi Setup	51
5.7	Algorithms Implementation	51
5.7.1	6-Step Drive Implementation	51
5.7.2	Field Oriented Control Implementation	51
6	RESULTS	53
6.1	BLDC	53
6.1.1	Voltage Waveforms	53
6.1.2	Current Waveforms	54
6.1.3	Voltage Control Plots	54
6.1.4	Current Control Plots	54
6.2	PMSM	55
6.2.1	Voltage Waveforms	55
6.2.2	Current Waveforms	55
6.2.3	Voltage Control Plots	56
6.2.4	Current Control Plots	56
7	CONCLUSION	57
7.1	Bla bla bla	57
7.2	Future Work	57
	BIBLIOGRAPHY	59
A	APPENDIX EXAMPLE: CODE LISTINGS	61
A.1	The listings package to include source code	61

## LIST OF FIGURES

---

Figure 1.1	Jedlik's "Electromagnetic Self-Rotor"	1
Figure 1.2	Rimac Concept S	3
Figure 3.1	Partially Assembled Motor	10
Figure 3.2	Lorentz's Law Diagram	11
Figure 3.3	Alignment Principle	13
Figure 3.4	DC Motor Scheme	14
Figure 3.5	DC Motor Electrical Model	15
Figure 3.6	Torque-Speed Curve	16
Figure 3.7	Brushless Motor Transverse Section	17
Figure 3.8	Different pole pair configurations	18
Figure 3.9	Electric Drive Scheme	20
Figure 3.10	Simple Three-Phase Inverter	21
Figure 3.11	Three-Phase Inverter	22
Figure 3.12	High-Side and Low-Side Driving Scheme	22
Figure 3.13	MOSFET Driving Diagram	23
Figure 3.14	Hall Effect Sensor	24
Figure 3.15	Sensorless Angular Detection	25
Figure 3.16	Shunt Resistance Current Detection	26
Figure 3.17	Trapezoidal BEMF	28
Figure 3.18	Six Step Commutation Currents	30
Figure 3.19	Six Step Commutation	31
Figure 3.20	PWM Signal	32
Figure 3.21	Sinusoidal BEMF	33
Figure 3.22	Electromechanical Dynamics Coupling	34
Figure 3.23	PI Controller	34
Figure 3.24	Speed Controller with Trapezoidal Drive	34
Figure 3.25	Torque Controller with Trapezoidal Drive	35
Figure 3.26	Field Oriented Control Blocks Diagram	36
Figure 3.27	Field Oriented Control applied in Speed Control	37
Figure 4.1	ROBI' Basic Configuration	39
Figure 4.2	Encoder Transmission Configuration	41
Figure 4.3	ECUs architecture	42
Figure 5.1	VESC Front Side	44
Figure 5.2	VESC Back Side	45
Figure 5.3	VESC Board Inverter	48
Figure 5.4	IRF 1	48

## LIST OF TABLES

---

Table 3.1	Six-Step commutating sequence	29
Table 4.1	HUB10GL in-wheel motor main characteristics	40
Table 4.2	Battery main characteristics	41

## LISTINGS

---

Listing A.1	Code snippet with the recursive function to evaluate the pdf of the sum $Z_N$ of $N$ random variables equal to X.	62
-------------	-------------------------------------------------------------------------------------------------------------------	----

## ACRONYMS

---

<b>BEMF</b>	Back Electromotive Force
<b>PMAC</b>	Permanent Magnet Alternating Current
<b>PMSM</b>	Permanent Magnet Synchronous Motor
<b>BLDC</b>	Brushless Direct Current
<b>PCB</b>	Printed Circuit Board
<b>FOC</b>	Field Oriented Control
<b>DC</b>	Direct Current
<b>PP</b>	Pole Pairs
<b>PWM</b>	Pulse Width Modulation
<b>MOSFET</b>	Metal–Oxide Semiconductor Field-Effect Transistor
<b>IGBT</b>	Insulated-Gate Bipolar Transistor
<b>ADC</b>	Analog-to-Digital Converter

<b>PI</b>	Proportional-Integral
<b>SPI</b>	Serial Peripheral Interface
<b>SSI</b>	Synchronous Serial Interface
<b>ECU</b>	Electronic Control Unit
<b>CAN</b>	Controller Area Network
<b>WMU</b>	Wheel Management Unit
<b>BMU</b>	Battery Management Unit
<b>VMU</b>	Vehicle Management Unit
<b>AMU</b>	Arm Management Unit
<b>FPU</b>	Floating Point Unit
<b>DSP</b>	Digital Signal Processor



## ABSTRACT

---

The purpose of this thesis is to study the architecture of a commercial brushless motor driving circuit proposed by Texas Instruments and implemented as an electronic speed board as an "open source" project available online, analysing the advantages and disadvantages of such design regarding the implementation of trapezoidal and sinusoidal motor driving and speed and current control techniques for an unmanned vehicle designed for robotic agriculture. After this, the implementation of such driving and control techniques was physically carried out and tested.

This thesis explains in details the most important parts regarding the physical implementation of a motor driving system in such a way that it can be fully replicated. Chapter 1 contains some initial information regarding the electric motor history and the motivation to realize this work. In Chapter 2, we explain more in detail the different reasons why this work was developed and the focus points that were stressed out. In Chapter 3, a simple but sufficient explanation about the theory behind the electric motor is given, explaining also the different existing technologies and their particular driving methods. In Chapter 4 we explain the study case of ROBI', a prototype mobile manipulator for agricultural applications, which uses the in-wheel motor for which the motor driver of this work was developed. In Chapter 5 we explain in deep detail all the work developed around the implementation of the motor driver, both in the software and the hardware fields. In Chapter 6 we explain the final results of the work, showing and comparing graphs and waveforms of the behaviour of the in-wheel motor driven by the system developed. Finally, on Chapter 7, we discuss the results of the work realized and propose a new system, based on the implementation of the researched architecture and the problems encountered while working on the project.



## ESTRATTO

---

Lo scopo di questa tesi è quello di studiare l'architettura di un circuito di guida del motore brushless commerciale proposto da Texas Instruments e implementato come un tabellone elettronico come un progetto "open source" disponibile online, analizzando i vantaggi e gli svantaggi di tale progetto per quanto riguarda l'implementazione di guida a motore trapezoidale e sinusoidale e tecniche di controllo di velocità e corrente per un veicolo senza pilota progettato per l'agricoltura robotica. Successivamente, l'implementazione di tali tecniche di guida e controllo è stata effettuata e testata fisicamente.

Questa tesi spiega in dettaglio le parti più importanti riguardanti l'implementazione fisica di un sistema di guida del motore in modo tale da poter essere completamente replicato. Chapter 1 contiene alcune informazioni iniziali sulla storia del motore elettrico e la motivazione per realizzare questo lavoro. Nel capitolo 2, spieghiamo più in dettaglio i diversi motivi per cui questo lavoro è stato sviluppato e gli aspetti principali che sono stati evidenziati. In Chapter 3 viene fornita una spiegazione semplice ma sufficiente sulla teoria alla base del motore elettrico, che spiega anche le diverse tecnologie esistenti e i loro particolari metodi di guida. Nel capitolo 4 spieghiamo il caso di studio di ROBI', un prototipo di manipolatore mobile per applicazioni agricole, che utilizza il motore a ruote motrici per il quale è stato sviluppato il driver motorio di questo lavoro. In Chapter 5 spieghiamo dettagliatamente tutto il lavoro sviluppato attorno all'implementazione del driver del motore, sia nel campo del software che in quello dell'hardware. Nel capitolo 6 spieghiamo i risultati finali del lavoro, mostrando e confrontando grafici e forme d'onda del comportamento del motore a ruote motrici guidato dal sistema sviluppato. Infine, in Chapter 7, discutiamo i risultati del lavoro realizzato e proponiamo un nuovo sistema, basato sull'implementazione dell'architettura ricercata e sui problemi incontrati durante il lavoro sul progetto.



## PREFACE

---

*Knowledge is only part of understanding.  
Genuine understanding comes from hands-on experience.*

— Seymour Papert *Constructionism* 1991

Motor control is a topic that must be experienced personally to be understood. This is a characteristic of many other engineering topics: they need to be experienced by the engineer or by the student to be fully understood. All the theory behind the movement of the shaft of the electric motor, which explains all the different phenomena interacting to create mechanical motion from electrical energy, should be experienced to fully understand everything that is involved. This is the reason why the practical implementation of theoretical topics is always interesting. Practical implementation makes us realize that there are always challenges that might not be taken into account while they are being studied from books, and they represent new opportunities to drive research and development for improvement.

This text was written with the idea of becoming a guide on the development of a motor controller for further projects, including the explanation of the basic physical phenomena that acts on electric motors and the important parameters to consider for the prediction of its motion, to the implementation of the hardware and software of a driving circuit and a detailed explanation on the most important factors to bring a motor controller alive and to successfully drive a permanent magnet motor. Even if the development of the work was intended for a specific project, all the information related to the development of the motor control systems can be applied to different projects, which is why this work can be useful also as a reference for projects not related to the robotic agriculture.

— Arturo Montúfar Arreola

## INTRODUCTION

*Electrical science, too, by its fascination, by its promises of immense realizations, of wonderful possibilities chiefly in humanitarian respects, has attracted the attention and enlisted the energies of the artist; for where is there a field in which his God-given powers would be of a greater benefit to his fellow-men than this unexplored, almost virgin, region, where, like in a silent forest, a thousand voices respond to every call?*

— Tesla On Electricity 1897

The electric motors made their first appearances in the middle of the XIX century right after the invention of the battery by the Italian physicist, chemist and inventor Alessandro Volta in 1800, the discovery of the generation of a magnetic field from an electric current by the Danish physicist and chemist Hans Christian Ørsted in 1820 and the invention of the electromagnet by the English physicist William Sturgeon in 1825 (Doppelbauer, 2012). After these foundations were laid, the development of a machine that generates mechanical power from electrical power has been improving day by day, and, along with that improvement, also its utility has been increasing.

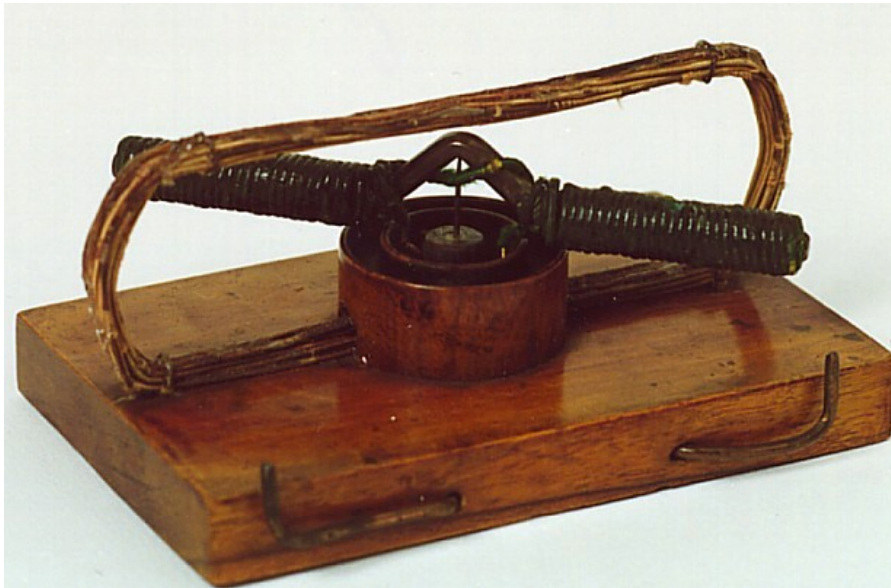


**Figure 1.1:** Jedlik's "Electromagnetic Self-Rotor". The historic motor created by the Hungarian physicist Ányos Jedlik still works perfectly today in the Museum of Applied Arts in Budapest.

Due to the reduction of the prices of metals and the improvement and automation of manufacture processes, electric motors became

available for a large range of applications, and not only as a research topic, up to the point that nowadays we interact with them in our daily life, sometimes without even noticing it. We have electric motors in all types of devices, from small applications like home appliances and hand-held gadgets, to large applications like robotics, cars and spaceships. As the complexity of the application increases, also the need for accuracy and efficiency does, leading to the development of more advanced electric motor technologies which lead to complex motion control techniques.

One of the most complex applications for motor control is robotics. The motion in a robotic system is part of its definition of automatic movement, therefore, a robotic system needs a predictable driving system to fulfil its purpose, which implies that most of the parameters of the motors inside the robot are known and that they can be controlled in a correct and precise way.

A challenging application regarding motors in robotics is the wheel driving, since it needs to be precise and powerful at the same time to transport the robotic system around large surfaces in an unmanned way, which means that there is no person on board and controlling the robot. For example, in robotic agriculture, which is one of the main reasons why this work was developed, a robot becomes an unmanned vehicle, which must transport itself around in farms, where the road represents harsh conditions for transportation, introducing the need for a precise drive to deal with small crops, a high torque to transport the robot in uneven grounds and a good range of speeds to displace itself in large field areas in the fastest way possible.

With aims to propose a solution for the land transportation in robotic agriculture projects, different types of motor technologies were studied a priori, finding out that in-wheel permanent-magnet brushless motors are one of the most suitable and currently used solutions to develop electric vehicles, since they don't need an external system for power transmission from the motor to the wheels, taking advantage of the high stall torque property of the electric motors and the reduction of the space and weight that having a motor inside a wheel represents (Bascetta, Baur, and Gruosso, 2017).

To correctly drive permanent-magnet brushless motors, it is necessary to apply a proper driving technique, which becomes a complex task when the goal is to achieve the desired characteristics mentioned previously: a good precision, a high torque and a large range of speed. Given such a challenge, the development of electric motor drives becomes one of the topics that draws the interest of many engineers and scientists, also due to the multidisciplinary approach needed to reach the speed, torque and efficiency required to drive the development that the inventions of tomorrow require. The approach to improve the motor drive in the electronics engineering field is directly related to the development of the driving circuit topology and to the imple-

mentation of complex control algorithms in embedded software that improve the performance of the different motor technologies available.

Since the brushless motor technology is quite recent in comparison with the rest, there is still a lot of development going on regarding its driving, with aims to reach the highest efficiency possible at the lowest cost. The objective of this work was to develop an electronic driver to control brushless motors, taking as a study case the in-wheel motors that transport a skid-steering robot designed for robotic agriculture. We studied the available electronic architectures to design a motor driver, the different approaches to drive brushless motors, like the trapezoidal and the sinusoidal drive and the peripherals needed to make these driving happen. After studying these topics, the motor driver was physically implemented and tested, and from this, a new architecture was proposed from the results and conclusions obtained from the implementation and testing of the circuit.



**Figure 1.2:** Rimac Automobili's electric supercar Concept S. Electric cars are becoming a trend and one of the main drivers for the development of technology related to electric motors.

This thesis explains in detail the most important information regarding the physical implementation of a motor driving system in such a way that it can be fully replicated. In Chapter 2, we explain more in detail the different reasons why this work was developed and the focus points that were stressed out. In Chapter 3, a simple but sufficient explanation about the theory behind the electric motor is given, explaining also the different existing technologies and their particular driving methods. In Chapter 4 we explain the study case of ROBI', a prototype mobile manipulator for agricultural applications, which uses the in-wheel motor for which the motor driver of this work was developed. In Chapter 5 we explain in deep detail all the work developed around the implementation of the motor driver, both

in the software and the hardware fields. In Chapter 6 we explain the final results of the work, showing and comparing graphs and waveforms of the behaviour of the in-wheel motor driven by the system developed. Finally, on Chapter 7, we discuss the results of the work realized and propose a new system, based on the implementation of the researched architecture and the problems encountered while working on the project.

# 2

## PROBLEM STATEMENT

---

As motion applications complexity increases, like in the robotics field, the need for a more complex and robust driving system arises, and with it, the need to make decisions regarding the technologies to be implemented for them. For example, when a robotics project begins, with the objective to implement a solution that hasn't been implemented before, one of the main concerns is the motion system. The selection of the motor that is going to be used in a project is not an easy task, since many details must be considered, like the speed and torque required by the application, which lead to the selection of the motor technology, which might be limited by the available power source, the computing power and the economic budget of the project. These aspects have a strong dependency between each other and choosing each one of them represents a trade-off that must be studied in detail to reach an optimal result for the desired application.

### 2.1 TECHNOLOGICAL TRADE-OFFS

One of the main goals in the technology research and development has always been to reduce the trade-offs between the most important parameters in different engineering applications, using the most suitable technologies available, depending on the application requirements. One of the fields of engineering that has a big focus on the reduction of trade-offs is the motor drive research, since their development is crucial to drive innovation in many engineering fields.

A complicated trade-off to deal with is the cost of a motor drive, which is one of the most limiting characteristics project developments, both for research activities and for industrial and consumer applications. If a project is not expected to generate an income after its development or it's not backed up by a research institute with resources, or if the product is expected to be kept at a low price for many different reasons (like accessibility for low income communities or the possibility of large expansion), the price of a motor drive might be the weak side in a trade-off analysis and the development of the project might not be optimal, since it might require more work to reach an acceptable result.

## 2.2 LEARNING CURVE

The cost of a project leads to another important trade-off on engineering research and development: the learning curve. In some areas like robotics, a professional engineering project requires thousands of hours of man-work to reach a desirable result. An important amount of the time available for these projects is used in learning theory regarding the technology related to the project and how the available tools for such technology work. This time consumed in learning all the information needed regarding a project is called “learning curve”. The amount of work necessary to reach a good result makes most of the engineering projects expensive and, in many cases, a big part of that time is consumed by the learning curve, time that could be used for developing another part of the project, increasing the speed of the development and, therefore, reducing its cost.

## 2.3 MOTOR DRIVER DEVELOPMENT

With the aim to solve these two important trade-off factors in motor driving systems, we decided to study the possibility to reduce the cost of a motor drive by using a driver based on a cheap architecture which can be easily modified and allows to understand in a fast way how the motor driver works, making the development around it faster and easier for future projects.

To set up the design specifications for the motor driver to be studied, we based the requirements in the drive characteristics of a robot designed for robotic agriculture designed by the engineering group of the AIRLab of the Politecnico di Milano called ROBI’ (Bascetta, Baur, and Gruosso, 2017). This robot is driven by four in-wheel brushless motors that will be described in detail in Chapter 4.

## 2.4 IMPLEMENTATION OF FIELD ORIENTED CONTROL

Having the objective defined, we looked for an already available platform to develop a motor driver with aims to look for points to improve and define a platform that could be used for different projects involving Permanent Magnet Alternating Current (**PMAC**) motors, both Brushless Direct Current (**BLDC**) and Permanent Magnet Synchronous Motor (**PMSM**). With this aim, we found a board called VESC Board, developed by the Swedish engineer Benjamin Vedder, who made available all the files for its production, including the schematic circuits, the bill of materials, the Printed Circuit Board (**PCB**) layout files and the source code. Vedder’s circuit was very appealing since it had many ports available and it was based on a technology that is easy to

study since it's based in a design proposed by Texas Instrument for three-phase motors.

Since this motor driver was needed to be used in robotics applications, we had the necessity to modify the source code of the microcontroller to apply motor control methods that would be different to the ones available for the VESC board since the code available was designed to drive an electric skateboard. For this aim, we decided to develop our own source code, this way we would have control over everything developed by us and the expansion of the code would follow up without the need of doing reverse engineering over the code that was already available.

Since the motors of the wheels of the robot are [PMSM](#), they have a sinusoidal configuration, and therefore, a sinusoidal waveform was needed to be applied into the motor to reach an optimal efficiency and to control the speed even in low speeds. This specification pointed us towards the implementation of the Field Oriented Control ([FOC](#)) method, which improves the torque capabilities of the motor at controlled low speeds as it will be explained in Chapter [3](#).



# 3

## MOTOR CONTROL THEORY

---

In this chapter, we will review some theoretical principles that concern us regarding motor control. First, we will review the physical principles that rule over the electric motors and we will explain the different motor technologies and its configurations, focusing in the Permanent Magnet Alternating Current (**PMAC**) motors. Later, we will review the motor drives, the configuration of a driver and the different driving techniques for the **PMAC** motors. Finally, we will explain the most common control methods that can be applied to them.

Most of the theory in this chapter was taken from the book *Tecnologie dei sistemi di controllo*, by Magnani, Ferretti, and Rocco, 2007 and from the compilation *Performance and Design of Permanent Magnet AC Motor Drives*, by Bose et al., 1989, as well as from the *Lecture notes in Power Electronics*, by Ghioni, 2016.

### 3.1 ELECTRIC MOTOR

An electric motor is an electric machine that transforms electrical power (product between voltage and current):

$$P_{electrical} = V \cdot I \quad (3.1)$$

into mechanical power (product between torque and angular speed):

$$P_{mechanical} = T \cdot \omega \quad (3.2)$$

by means of the electromagnetic phenomena that takes place inside the motor, which is explained by the physical principles mentioned in this chapter.

#### 3.1.1 Physical Principles

The generation of torque in electric motors is based in the interaction of two magnetic fields, one generated by magnets or windings placed in the stator and the other one generated by magnets or windings placed in the rotor as seen in Figure 3.1.

The physical laws that rule over the torque generation in the electric motor are mainly four: The Lorentz's Law, which helps us define the torque generated by an electric charge moving inside a magnetic field; Faraday's Law of Electromagnetic Inductance and the Lenz's Law,

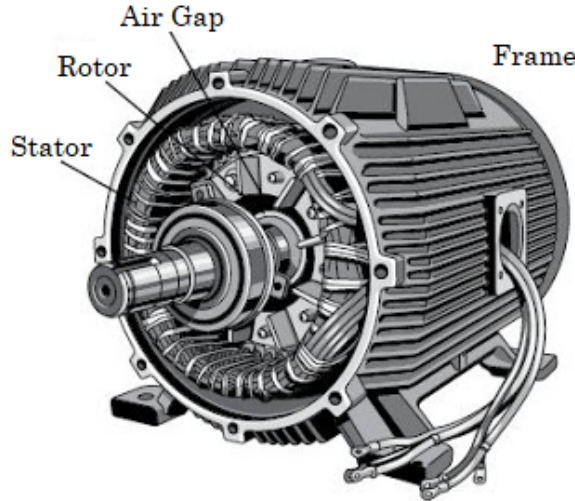


**Figure 3.1:** Partially Assembled Motor. An electric motor consists mainly in three parts: a rotor, which moves due to the electromagnetic interaction; a stator, the body of the motor; and a frame, which holds the rotor and the stator together. The air gap is the space between the rotor and the stator, where the electromagnetic interaction takes place (*Electrical Motors Basic Components*, 2012).

which explain the generation of the Back Electromotive Force (BEMF) in the motor coils depending on the speed of the rotor and the influence of the magnetic field generated due to this BEMF respectively; and the Ampere-Laplace Law, which allows us to calculate the magnetic field of a current loop and the mechanical interaction between two magnetic fields.

LORENTZ'S LAW defines a force  $F$ , which acts over an electric charge  $q$  moving with a speed  $v$  inside a magnetic field with intensity  $B$ :

$$F = qv \times B \quad (3.3)$$

as seen in Figure 3.2. By defining a current  $I$  passing through a conductor with length  $l$  we can transform Equation 3.3 into Equation 3.4:

$$F = lI \times B \quad (3.4)$$

Considering the current  $I$  flowing through a conductive loop as the one in Figure 3.2 with sides lengths  $l$  and  $h$  we can see that there is a force  $F$  generated in the direction of the cross product of the current  $I$  and the magnetic field  $B$ . The maximum force  $F$  is generated in the sides of the loop where the direction of the

current  $I$  is perpendicular to the direction of the magnetic field  $B$  ( $ab$  and  $cd$ ), while on the other two sides ( $ad$  and  $bc$ ) the forces generated are cancelled with each other due to the direction of the current respect to the magnetic field.

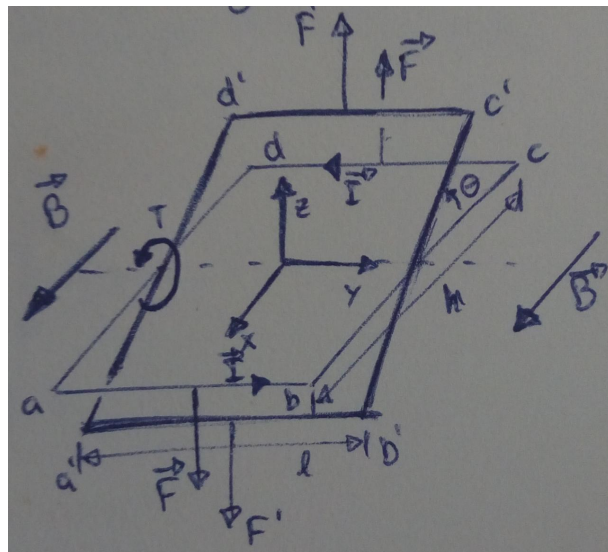


**Figure 3.2:** Visual explanation of the interaction of the current  $I$  and the magnetic field  $B$  generating a force  $F$  and, consequently, a torque  $T$  around the  $y$  axis (Magnani, Ferretti, and Rocco, 2007).

Since the forces  $F$  generated on the sides  $ab$  and  $cd$  have the same magnitude but different direction, they create a torque  $T$  around the  $y$  axis defined by the magnetic field, the current and by the length of the sides of the loop as:

$$T = IhlB \cos \theta \quad (3.5)$$

We can see in Figure 3.2 and in Equation 3.5 that when the angle  $\theta$  between the sides  $ad$  or  $bc$  and the direction of the magnetic field  $B$  is  $\pi/2$  radians, the torque  $T$  is zero and when the angle  $\theta$  is zero or  $\pi$  radians, the torque reaches its maximum possible value.

The dependency of the torque created by the interaction of the current and the magnetic field on the angle between these two physical quantities introduces the need of changing the direction of the magnetic field or the direction of the current, hence, the polarity of the loop, to maintain the loop spinning and a non-zero torque.

FARADAY'S LAW OF ELECTROMAGNETIC INDUCTION states that

In every circuit under the effect of a magnetic field, an electromotive force is induced equal to the deriva-

tive respect to the time of the magnetic flux passing through the circuit, with negative sign (Jordan, 1968).

therefore, by indicating with  $E$  the electromotive force and with  $\phi_m$  the magnetic flux, we have:

$$E = -\frac{d\phi_m}{dt} \quad (3.6)$$

If we consider a case like the one in Figure 3.2 we can calculate the magnetic flux passing through the loop as:

$$\phi_m = B \cdot u_N S = B \cdot u_N h l = h l B \sin \theta \quad (3.7)$$

where  $S$  is the surface of the loop and  $u_n$  is the direction normal to the plane of the loop. Therefore, we get an induced electromotive force of:

$$E = -\omega h l B \cos \theta \quad (3.8)$$

where  $\omega$  is the angular speed of the loop. We can see, comparing Equation 3.8 and Equation 3.5, that the induced electromotive force depends on the angular speed in the same way than the acting torque depends on the current.

**LENZ'S LAW** can be explained after the explanation of the induced electromotive force. It states that the induced current in a loop has the direction that creates a magnetic field that opposes the change in magnetic flux through the area enclosed by the loop, therefore, the induced current tends to keep the magnetic flux  $\phi_m$  from changing in the circuit.

If the rotation of the loop is generated by the circulation of a current inside a magnetic field, the induced electromotive force will try to oppose to the pass of the current, that's why it's normally referred to as Back Electromotive Force (**BEMF**).

**AMPERE-LAPLACE LAW** is the last piece to understand the transformation of electrical energy into mechanical energy. It allows us to calculate the magnetic field generated by a closed loop conducting current in a point defined by a vector  $p$  as:

$$B(p) = \frac{\mu_0}{4\pi} \oint I \frac{u_t \times u_r}{r^2} dl \quad (3.9)$$

where  $\mu_0$  is the vacuum magnetic permeability constant,  $I$  is the current circulating through the loop,  $u_t$  is the versor with

direction of the current in the infinitesimal element  $dl$  and  $u_r$ , and  $r$  are versor and module that define the point  $p$  respect to the infinitesimal element of the loop.

Given that the magnetic fields can be generated both by permanent magnets and by current circulation, the electromechanical conversion is obtained due to the interaction of two magnetic fields according to the alignment principle, which states that

In a region of space which hosts two magnetic fields, there is a mechanical action that tends to align both fields. (Magnani, Ferretti, and Rocco, 2007)

If we consider the loop from Figure 3.2 and Equation 3.9, we can see that there is a magnetic field generated around the loop as seen in Figure 3.3, and due to the alignment principle, we will get the strongest coupling torque when the magnetic fields are perpendicular to each other.

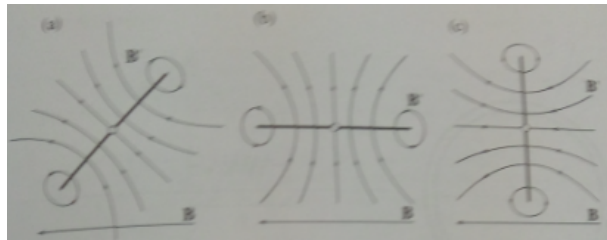


**Figure 3.3:** Visual explanation of the alignment principle. The alignment torque is the largest in the configuration of figure B and nule in the configuration of figure C.

In the case of electrical motors, there are two different magnetic fields generated in the airgap due to the permanent magnets or to the windings placed in the stator and the rotor which can be considered in radial direction, described by two magnetic fields  $B_r(\theta, t)$  and  $B_s(\theta, t)$ , from which interaction we get the electromechanical conversion, since we have the generation of a torque which tends to align the two fields angles where they have the largest intensity. The alignment torque will be an expression of the type:

$$T_m = k B_r B_s \sin \delta \quad (3.10)$$

where  $\delta$  is the de-phasing angle between the two fields and the maximum torque will be when  $\delta = \pi/2$ . In conclusion, by feeding the windings in the right way, we look forward to having a constant  $90^\circ$  de-phase between the two magnetic fields in aims to obtain the maximum torque generation.

In the case of the Direct Current (DC) motor, the perpendicularity condition between the magnetic fields is maintained by a polarity

commutating structure attached to the rotor which is connected to the windings where the current flows and generates the rotor magnetic field that tries to align itself to the magnetic field of the permanent magnets attached to the stator. This commutating system is connected to the power supply by means of metallic brushes that energise the motor until it reaches a certain angular position and the commutating lead changes to the next one, changing the polarity of the windings. Therefore, the torque obtained is independent from the position of the rotor and it's proportional to the amplitude of the power source.

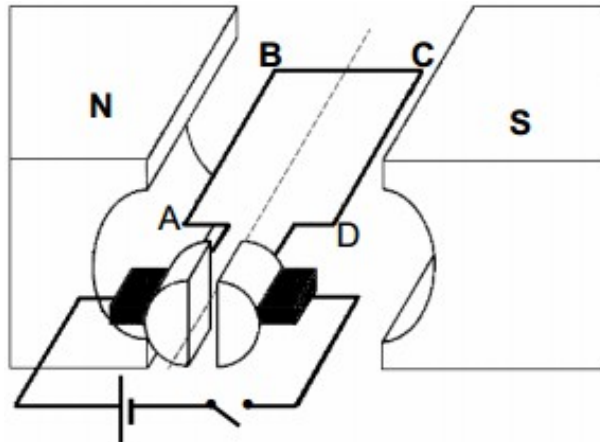


**Figure 3.4:** Basic schematic representation of the DC motor using the same loop represented in Figure 3.2

In brushless motors, which will be explained later in this chapter, the perpendicularity condition is maintained by feeding in the right time the windings in function of the angular position of the rotor  $\theta$ .

Finally, after all the electromechanical phenomena that interacts inside the motor has been explained, we can obtain the electromechanical conversion between  $P_{\text{electrical}}$  and  $P_{\text{mechanical}}$ .

If we clear from Equation 3.5, the torque  $T$  and the current  $I$ , grouping the rest of the variables into one constant, we can write down the following equation:

$$T = K_T I \quad (3.11)$$

where  $K_T$  is called Torque Constant and is defined by the geometry of the motor and the magnetic field in the airgap of the motor, which depend on the motor configuration and its construction technology.  $K_T$  units are  $Nm/A$ .

We can do the same with Equation 3.8, clearing the BEMF and the angular speed  $\omega$ , getting the following equation:

$$BEMF = K_E \omega \quad (3.12)$$

where  $K_E$  is called Voltage Constant and it's defined also by the type of motor we are using.  $K_E$  units are  $V/(rad/s)$ .

If we consider the loop of Figure 3.2 as an equivalent circuit like the one in Figure 3.5, where the inductance  $L$  is generated due to the windings of the coil into the rotor, and  $R$  is the resistance of the conductive material, we can write the Kirchhoff's Voltage Law on its terminals as:

$$v(t) = Ri(t) + L \frac{di(t)}{dt} + bemf(t) \quad (3.13)$$

which at steady state, when the current is constant, becomes:

$$V = RI + BEMF \quad (3.14)$$

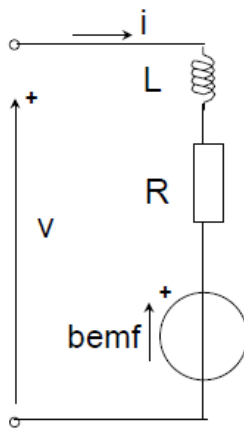


**Figure 3.5:** Equivalent circuit representation of a motor winding.

We can write down that the net power input into the circuit of Figure 3.5,  $VI - RI^2$ , is equal to the electrical power absorbed by the BEMF:

$$P_{electrical} = BEMF \cdot I = K_E \omega I \quad (3.15)$$

and we can also see that the mechanical power can be written using these new constants:

$$P_{mechanical} = T \cdot \omega = K_T I \omega \quad (3.16)$$

The two constants,  $K_E$  and  $K_T$ , synthesize the most important parameters used in the electromechanical power conversion in an electric motor. If we impose a voltage difference between the terminals of the loop of Figure 3.5, we create a current  $I$  that depends on the loop

impedance. From Equation 3.11, we can see that such current will generate a proportional torque  $T$ . In the same way, from Equation 3.12, we obtain that the BEMF generated by the movement of the coil, due to the generated torque, will define a proportional angular speed  $\omega$ . If we rearrange the terms from Equation 3.14 using Equations 3.11 and 3.12, we can see the interrelation between the rotating speed of the motor  $\omega$  and the torque  $T$  being generated:

$$\omega = \frac{V}{K_E} - \frac{R}{K_T K_E} T \quad (3.17)$$

which defines, by imposing a voltage difference between the terminals of the loop, the torque  $T$  vs angular speed  $\omega$  curve that characterizes the mechanical behaviour of an electrical motor.

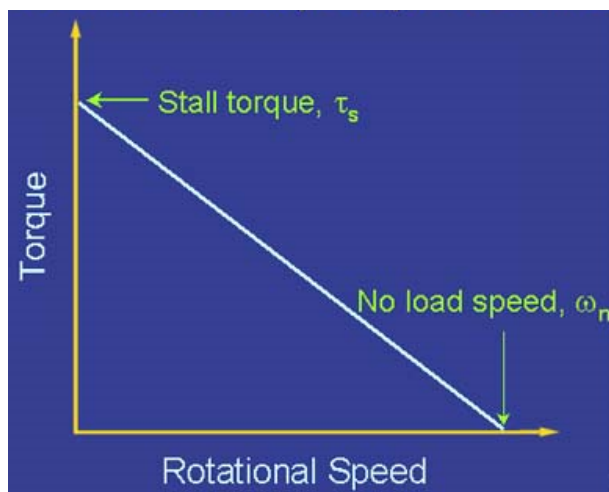


**Figure 3.6:** Basic representation of the Torque vs Angular Speed characteristic curve of an electric motor

If the speed of the motor  $\omega$  is equal to zero, then we can rearrange the terms and see that the torque  $T$  is defined by  $K_T V / R$ , which is the maximum torque that the electric motor can provide by a given voltage, also named Stall Torque,  $T_0$ . We can also define a no-load speed  $\omega_0$ , for the case when there is no load influencing over the movement of the rotor, as  $V / K_E$ .

The relationship between torque and angular speed established in Equation 3.17 will help us select the voltage that we need to regulate in order to control the dynamics of the motor.

It is important to mention that these equations also work if there is an imposed angular speed  $\omega$ . If we impose an angular speed to the rotor, the motor works as a voltage generator:

$$V = K_E \omega + R \frac{T}{K_T} \quad (3.18)$$

therefore, if we connect the motor to a load, it generates a voltage proportional to the driving speed and provides a current proportional to the torque driving the rotor. This behaviour is used in the so-called regenerative braking, since we can obtain energy when we want to stop a motor which is moving due to an inertial torque.

### 3.2 PMAC MOTORS

The Permanent Magnet Alternating Current (**PMAC**) motor is a type of electrical motor that doesn't need the mechanical commutators mentioned in [3.1.1](#) to be driven as in the case of the DC motor, but its windings need to be energised in a specific sequence to commutate and function correctly by means of an inverter. Since it doesn't need the mechanical commutators, it also doesn't need the brushes that energise the windings, so it can be said that it's a brushless motor. As seen in Figure [3.7](#), there are permanent magnets attached to its rotor. The stator consists of stacked steel laminations on which the coils are wound in a three-phase configuration.

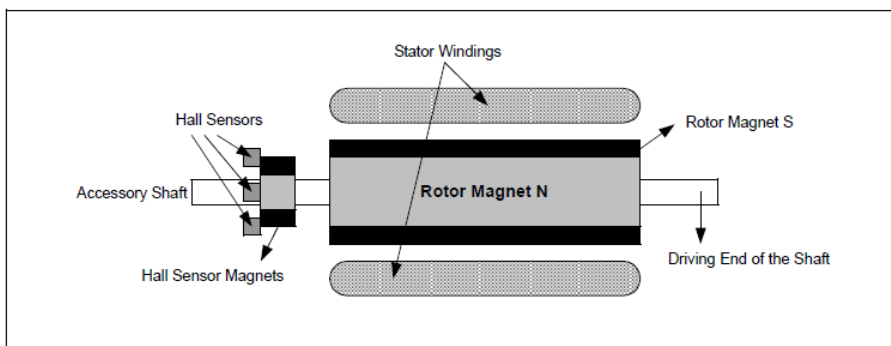


**Figure 3.7:** Brushless motor transverse section ([microchip microchip](#)).

These three phases are feed alternatively in such a way that the magnetic field, generated by the relative currents passing through the coils, should always be orthogonal and synchronous to the magnetic field generated by the rotor's permanent magnets. The characteristics mentioned above give the name to this kind of motors.

To maintain the synchronization, it's necessary to commute, by means of an inverter, the currents in the windings of the stator, taking as a reference the angular position of the rotor, which must be obtained by a sensor.

The number of commutations needed to generate one revolution of the rotor is determined by the number of magnetic Pole Pairs (**PP**) of the permanent magnets attached to the rotor. One **PP** is defined by 2 magnets attached to the rotor, one with the north pole facing out in one side of the rotor and one with the south pole facing out in the opposite side of the rotor. Normally, the **PMAC** motors have many **PP** (four or more) in order to have a lower torque ripple since the align-

ment of the magnetic fields would be every  $360 / (\text{PP} \times \Phi_N)$  degrees of the rotor, where  $\Phi_N$  is the number of phases in the motors. For the electromechanical conversion, the angular position of the rotor is substituted by an electrical angular position, which is controlled by the commutator and is defined by:

$$\theta_{\text{electrical}} = \text{PP} \cdot \theta_{\text{mechanical}} \quad (3.19)$$

which also represents a relationship between the mechanical speed of the rotor and the electrical speed of commutation, which is defined by the commutation frequency:

$$\omega_{\text{electrical}} = f_{\text{commutation}} = \text{PP} \cdot \omega_{\text{mechanical}} \quad (3.20)$$

so, for example, if we have a motor with 6 PP and we want to drive it at 1kHz, we must commute the polarity of the inverter at

$$f_{\text{commutation}} = \text{PP} \cdot \omega_{\text{mechanical}} = (6)(1\text{kHz}) = 6\text{kHz} \quad (3.21)$$

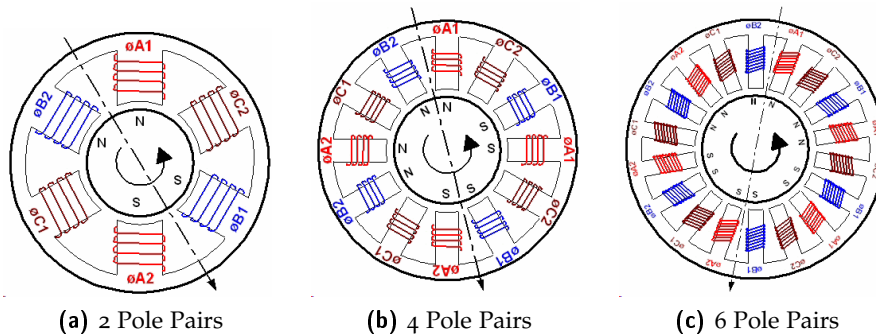


**Figure 3.8:** Different pole pair configurations

The main characteristics that make the brushless motor a better option for some applications than the DC motor are the following:

- better weight-to-power ratio,
- a more linear acceleration,
- a low inertia,
- a higher reliability,
- smaller dimension,
- reduced need for maintenance,
- high rotation speed,

- ideal for working in hostile environments

but there are two disadvantages to this motor technologies:

- need of a rotation sensor,
- need of a complex logic to commutate the currents flowing through the coils

Both of these disadvantages are mainly reflected in a higher price respect to the **DC** motor.

It is possible to identify mainly two types of brushless motors. The first one is the Brushless Direct Current (**BLDC**) motor, which has a rotor position feedback that is not continuous, since the position of the rotor is given every 60 electrical degrees and its feed in blocks of 120 electrical degrees by simply alternating the voltage in the inverter, and due to these alimentation in blocks, the driving is rectangular, so the ideal **BEMF** is trapezoidal. The second type of brushless motors is called Permanent Magnet Synchronous Motor (**PMSM**), and it needs a continuous rotor position feedback to feed the motor with sinusoidal current, obtained by Pulse Width Modulation (**PWM**) of the **DC** bus, therefore the ideal **BEMF** is sinusoidal, which generates a lower torque ripple than the trapezoidal one, but needs a more complex control method.

### 3.2.1 BLDC Motors

The stator winding for each one of the three phases of the **BLDC** motor consists of a uniform distribution of turns over  $N = \text{PP}$  sectors of a width equal to  $60^\circ$ . The magnets attached to the stator cover an arc of  $180^\circ$ , and at any instant, each magnet interacts, for  $120^\circ$ , with an arc of stator conductor carrying current.

Due to this "discrete" interaction every  $120^\circ$ , the three-phase switching between the currents of the stator should happen when the edge of the magnet attached to the rotor reaches the boundary between windings every  $60^\circ$ , therefore, a trapezoidal **BEMF** is generated in its coils.

The boundary of the rotor magnets with respect to the windings position is detected by three sensors, one every  $120^\circ$ , which send a signal to the driving circuit to change the polarity of the coils depending on the actual value of the three sensors and on the desired direction. The sensors to detect the angular position will be explained in [3.3](#) and the driving sequences will be explained in [3.4](#).

### 3.2.2 PMSM Motors

The stator of the **PMAC** motor is fitted with three-phase windings with  $N = \text{PP}$  turns of each phase distributed sinusoidally around

the periphery. If the stator windings are feed by sinusoidal currents, there is a linear current density around the stator periphery and a sinusoidal **BEMF** is generated in its coils.

Since the sinusoidal feeding of the current into the coils depends continuously on the magnetic field of the rotor permanent magnets, it is necessary to use an angular position sensor attached to the rotor. The sensors to detect the angular position will be explained in 3.3 and the driving algorithm will be explained in 3.4.

### 3.3 ELECTRIC DRIVES

An electric drive can be defined as an electromechanical device that converts electrical energy into mechanical energy to impart motion to different machines and mechanisms for various kinds of process control (*Ghoni Introduction to Electrical Drives*).

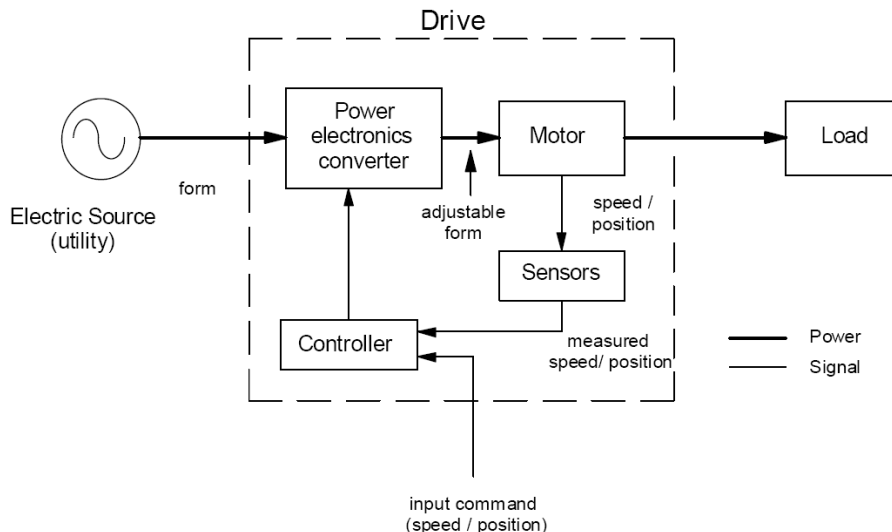


**Figure 3.9:** Electric Drive Scheme

The brushless motor drive, therefore, consists not only on the electric motor and the inverter, but it also includes the position, speed and current feedback systems, these being external sensors, embedded circuits or just algorithms, the vector, current, speed and position controllers and the DC power supply which can be a battery for mobile applications or a rectified power source for industrial applications.

### 3.3.1 Inverter

The commutation of the polarities in the windings of the PMAC motors is done by means of a three-phase inverter. The inverter used in

PMAC motors avoids the need of the mechanical commutation used in the DC motors, which creates sparks between the commutator and the brushes due to the discharge of the electromagnetic energy stored in the windings of the rotor.

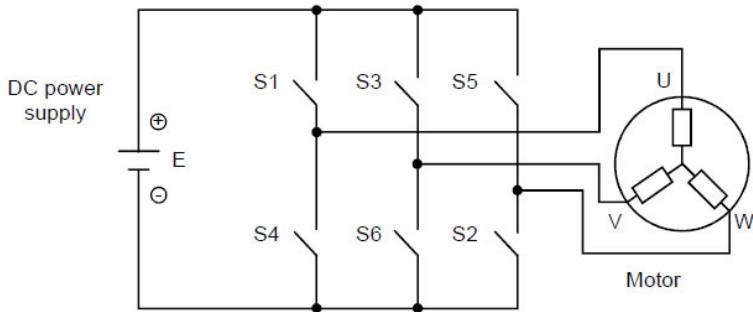


**Figure 3.10:** Schematic representation of a three-phase inverter

This three-phase inverter configuration consists on 3 branches with 2 switches each one. The middle point between the two switches in each branch is connected to each one of the phases of the motor. To feed the coils of the motor, we need to activate the switches in such a way that the current comes into one of the phases and comes out through another phase. For example, if we want to feed a current through phase  $U$  and we need it to come out through phase  $V$  to generate a magnetic field in a certain angle, we would enable switches  $S1$  and  $S6$ , having a phase-to-phase voltage in the  $U$  and  $V$  coils equal to  $V_{DC}$ . The correct feeding sequence should be synchronous with the rotor position to generate an angular rotation of the rotor with the lowest possible torque ripple.

The switching in the three-phase inverter is made by transistors as seen in Figure 3.11. The transistors are chosen accordingly to the power requirements of the application on which the inverter is being used. If the DC voltage is lower than 1000V and the current is lower than 100A, it is recommended to use the Power Metal–Oxide Semiconductor Field-Effect Transistor (MOSFET) technology. If the power consumption of the motor is larger, different technologies should be considered, like the Insulated-Gate Bipolar Transistor (IGBT).

The use of recirculation diodes is necessary to avoid damage in the transistors due to the overvoltage generated by the current transients in the windings  $LdI/dt$  that takes place between the switches of a same branch of the inverter while switching from one state to another. For example, when a transistor is suddenly turned off, the current flowing through the coils doesn't instantly disappear, but instead it recirculates through the diodes until it vanishes.

Since Power MOSFETs have large parasitic capacitances, they can't be driven by typical CMOS (0 to 3V) or TTL (0 to 5V) logic signals, which typically have a low current driving capability. Instead, to drive a power MOSFET is necessary to use a more complex driving circuit to

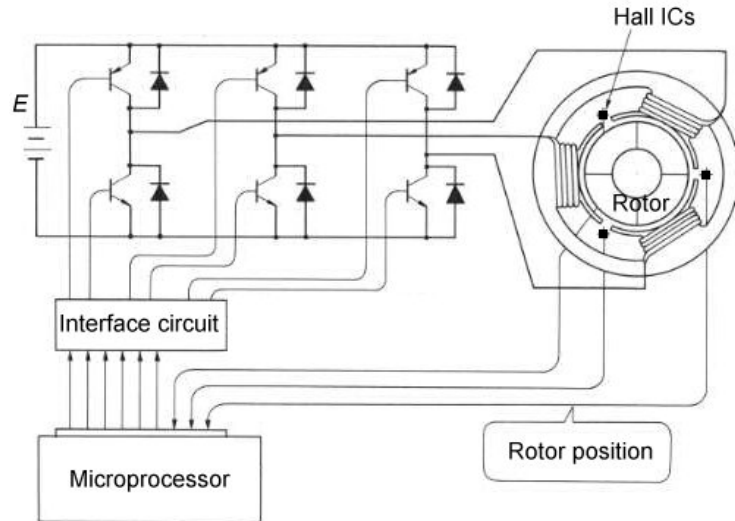


**Figure 3.11:** Schematic representation of a three-phase inverter built with transistors

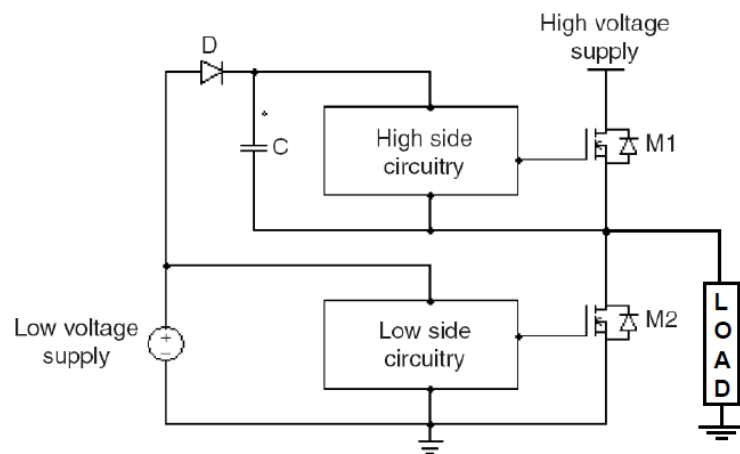


**Figure 3.12:** Power MOSFET devices require a dedicated circuit to provide enough voltage and current to drive their gates

rapidly charge the capacitance of the gate and reach a value of  $V_{GS}$  large enough to switch the device. Some integrated circuits provide solutions to solve this problem. These integrated circuits can be considered as part of the inverter, because without them, the inverter won't be driven correctly.

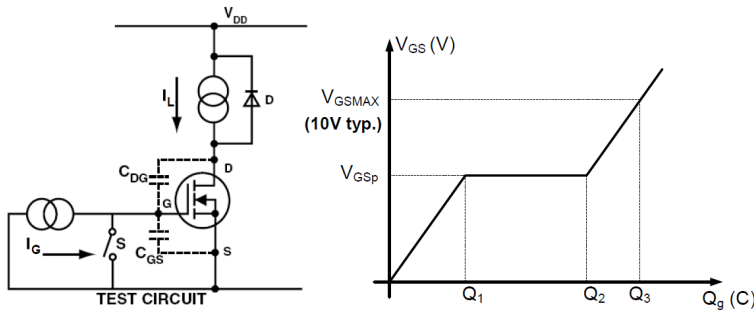


**Figure 3.13:** Schematic representation of the components influencing on the driving of a Power MOSFET

### 3.3.2 Angular Position Sensors

It is strictly necessary to obtain the angular position of the rotor in order to energise the coils of a [PMAC](#) motor in a synchronous way. The angular position detection can be made in different ways, but the solutions are mainly separated into two groups: sensored and sensorless.

The sensored angular detection is made by an external device, which creates a signal that allows us to know the angular position of the rotor. Typically two different approaches are used for the sensored angular detection. The first approach, and the simplest one, is the use of Hall effect sensors. Hall effect sensors are transducers that variate an output voltage signal in response to a magnetic field acting over them, and depending on their configuration the output can be digital (high or low signals) or analog (the output voltage variates proportionally to the detected magnetic field strength). In the case of the brushless motors, since the rotor has permanent magnets attached to it, three Hall effect sensors are mounted inside the motor frame in order to read the magnetic field of those permanent magnets and create a digital output that helps us determine the angular position of the rotor. The Hall effect sensors are mounted every 120 electrical degrees, so they can be mounted in different positions around the rotor, but they will change the output signal every 60 electrical degrees, depending on the pole orientation of the rotor. This approach is mainly used in [BLDC](#) motors, since they are winded in a trapezoidal distribution with aims to use only these simple sensors and an inverter.

The second approach to the sensored angular detection is the use of absolute rotary encoders. These encoders are attached to the shaft of

the motor and, therefore, provide the angle of the rotor continuously. There are different technologies used for this approach. The simplest one is the resistive encoder, which is practically a potentiometer attached to the rotor's shaft, so it is prone to mechanical disturbances and noise, but is very cheap. The next approach is the optical encoder, which identifies the absolute angular position by means of attaching a disk with holes or with a pattern and optical sensors, like infrared LEDs and infrared detectors. The optical encoder is a very precise approach, but is very prone to mechanical disturbances, so it is mostly used in applications where the conditions to the system don't represent a problem to the encoder. The approach that is being used in this project to detect the absolute angular position is the magnetic encoder, which also uses Hall effect sensors for the absolute angular position determination. The difference between these two approaches is that, in this case, the Hall effect sensors of this encoder provide an analog signal proportional to the angular position of the magnetic field of an external permanent magnet, which is attached to the shaft. Another interesting technology that is being used recently is the capacitive encoder, which detects the capacitance changes, proportional to the angular position, using a high frequency reference signal. The absolute angular position detection is used mainly in the [PMSM](#) technology, since it is necessary to know the angular position of the rotor continuously to create a sinusoidal signal, to drive the sinusoidally distributed coil windings, synchronously to the magnetic field of the permanent magnets attached to the rotor.

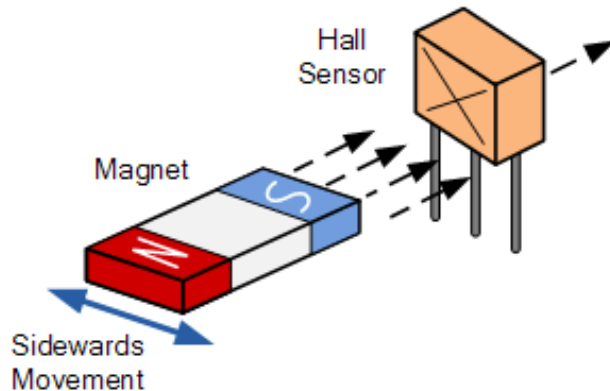


**Figure 3.14:** Hall Effect Sensor

One important thing that has to be considered when using absolute rotary encoders is that, even if these encoders provide the absolute angle of the rotor, they don't necessarily provide the angular position of the magnetic field of the rotor, introducing an angular slip  $\Delta\theta$  which is equal to the difference between the value of the absolute rotary encoder angle and the angular position of the magnetic field. For this reason, the three Hall effect sensors used in the first sensed approach can be found also in [PMSM](#) motors and not only in [BLDC](#) mo-

tors, since they can provide the exact position zero of the magnetic field of the permanent magnets.

The sensorless approach to obtain the angular position of the rotor consists in reading the **BEMF** on an undriven motor terminal during one of the drive phases. This is done by means of connecting a voltage divider to the middle point of each inverter branch, in order to read the analog voltage signal proportional to the **BEMF** and calculate the angular position of the rotor. This solution can be used for both **BLDC** and **PMSM** technologies. The sensorless approach reduces the size and the cost of the motor drive, and it's also useful in applications where the rotor runs immersed in fluid. Even if this method is more complex than just reading the angular position, the main disadvantage is that the motor must be rotating at a minimum rate to generate a **BEMF** that can be detected by the controller, therefore, this approach is not convenient in applications where a motor must run at low speeds.

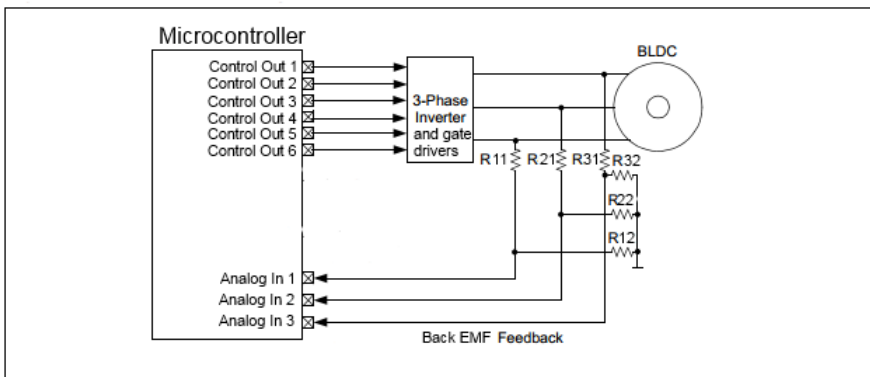


**Figure 3.15:** Sensorless Angular Detection Circuit

### 3.3.3 Current Sensors

Knowing the amount of current that is circulating through the motor windings can help us apply different control strategies to control the torque as defined in Equation 3.11. Also, reading the current can help us avoid problems of overcurrent if something goes wrong with the motor drive system.

To read the current we must install an external sensor which can be as complex as the application requires and the budget allows. The simplest approach to measure current, which is also the approach used in this project, is the use of a shunt resistor. The shunt resistor is an electrical resistor with a low (but well controlled) resistance value. This shunt resistor is placed in the path of the current flow of the motor's coils, in such a way that when the current flows through

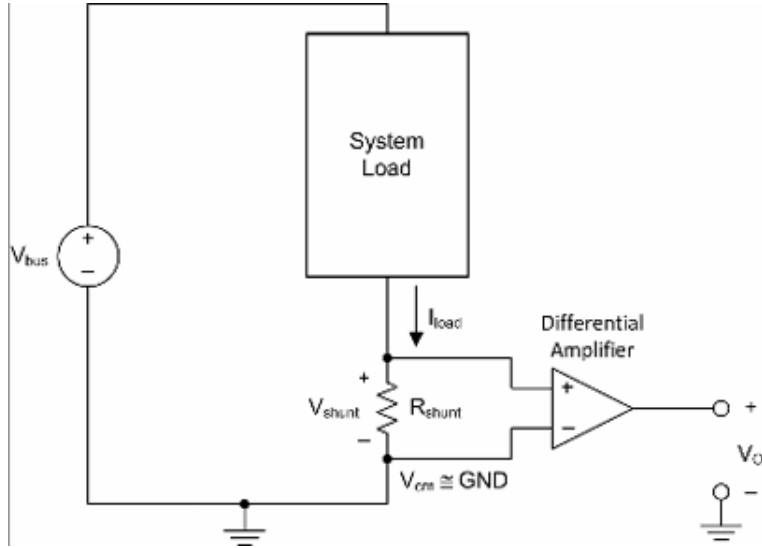


**Figure 3.16:** Measurement of the current flowing through a load using a shunt resistance

the resistor, we have a proportional voltage drop across it following Ohm's Law:

$$I_{phase-to-phase} = \frac{V_{shunt}}{R_{shunt}} \quad (3.22)$$

Since we need to take care of the power dissipated in the shunt resistor  $P_{shunt} = I^2 R$ , small resistance values  $R$  with large power dissipation capability are selected, leading to the problem that this generates a proportional voltage signal that is very small and that is prone to noise disturbances. For example, if we have a current of  $100mA$  flowing through a shunt resistance of  $0.001\Omega$ , we would get a voltage drop across the shunt resistance equal to  $0.1mV$ , which is a very small value to be read by a typical Analog-to-Digital Converter ([ADC](#)). To solve this problem, we need to include an amplifier that allows us to read such a small voltage with a normal [ADC](#), therefore, we can calculate the equivalent current as:

$$I_{phase-to-phase} = \frac{V_{amplifier}}{R_{shunt} G} \quad (3.23)$$

where  $G$  is the gain of the voltage amplifier.

### 3.3.4 Controller

The last piece on the motor drive is the controller, which executes all the logic behind the commutation of the inverter, in order to generate a synchronous driving. Previously, motor controllers were made

by analog electronic circuits. Nowadays, these controllers are implemented using digital circuits that can be programmed, like microcontrollers.

The microcontroller has the task to run the logic that generates a driving signal for the inverter which will depend in the desired dynamic conditions and the actual conditions of the motor, which are sensed and stored by the microcontroller.

For example, if we need to drive a motor at a desired reference speed, we need to apply a synchronous voltage signal into its coils. To generate a voltage that is synchronous to the angular position of the magnetic field, we will need to start by defining the absolute angular position of the shaft and, after this, we can apply a voltage into the coils by switching on the respective transistors of the inverter. This voltage will generate a current that will generate a torque and a magnetic field that will interact with the rotor, starting to spin it and, with this, generating a **BEMF**. As the rotor spins, we must keep reading its angular position, to determine the correct driving voltage needed to keep it spinning and the correct commutation of the transistors in the inverter. As the motor keeps moving, everytime faster, we need to calculate the speed at which the rotor is spinning, so as the rotor approaches the desired angular speed, we must increase or reduce the commutating frequency of the inverter, closing the speed loop. All these tasks must be made automatically by the microcontroller in a matter of microseconds.

The microcontroller handles also the interface between other devices, allowing us to modify control parameters, like the desired speed or torque, and to read different physical variables from the motor drive that are detected by the system.

### 3.4 PMAC MOTORS DRIVING METHODS

Due to the different configurations of the coils between **BLDC** and **PMSM** motors, there are two methods to apply a voltage into the coils, depending on the generated **BEMF**. To obtain the best torque using a simple driving method in **BLDC** motors, we can apply the Trapezoidal Driving method, which is the driving method for which **BLDC** motors are designed. This method can also be used in the **PMSM** motors, but it won't allow us to obtain the best torque available for this motor technology. To obtain a better torque in both motors, we can apply the Sinusoidal Driving method, which allow us to have a better current density, mainly in the **PMSM** motor.

#### 3.4.1 Trapezoidal Drive

The trapezoidal drive is intended to create a trapezoidal **BEMF**, as the name indicates, by energising positively one of the windings, connect-

ing it to  $V_{DC}$  (current comming in), and negatively a second winding, connecting it to 0V (current going out), while the third winding remains floating (no current flowing through it), using the three-phase inverter explained in 3.3.1. This energising will generate a magnetic field in a certain angle that will interact with the magnetic field of the rotor, producing a torque between the rotor and the stator and, therefore, a rotation of the rotor if the load is smaller than the torque generated. The sequence of commutation that is followed to create the trapezoidal BEMF is called "six-step" commutation.

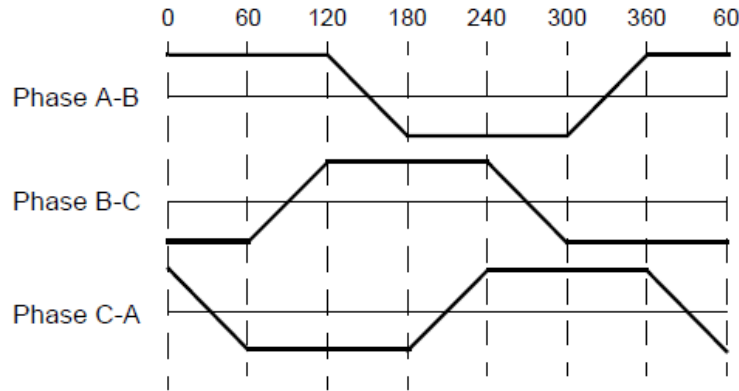


Figure 3.17: Trapezoidal BEMF

The six-step commutation is produced by following the sequence described in Table 3.1, which depends on the rotor position, which is defined by the Hall effect sensors, and on the expected direction of rotation. This sequence generates a current circulation like the one explained in Figure 3.18, which produces a BEMF and a torque like the one shown in Figure 3.19. We can see that the torque in Figure 3.19 presents a ripple due to the non-continuous shape of the current in the coils, generated by the rectangular commutation of the six-step sequence. This current shape is defined by the electrical model of the coils of an electric motor, which follows a model similar to the one described in Figure 3.5 and Equation 3.13.

Due to the synchronous configuration of the PMAC motors, the six-step commutation frequency is defined by the rotation speed and not vice versa, unlike in induction motors. Instead, to reduce the rotation speed, we need to reduce the current flowing through the windings by reducing the voltage applied into the windings, following Equation 3.17. To achieve this with the inverter, we must follow the six-step sequence applying a PWM signal into the gates of the transistors with a frequency higher than the inverse of the time constant  $\tau = L/R$  of the motor, which is much higher than the six-step commutating frequency. By doing this we apply an average voltage  $D \cdot V_{DC}$  into the windings, where  $D$  is the duty cycle of the PWM signal.

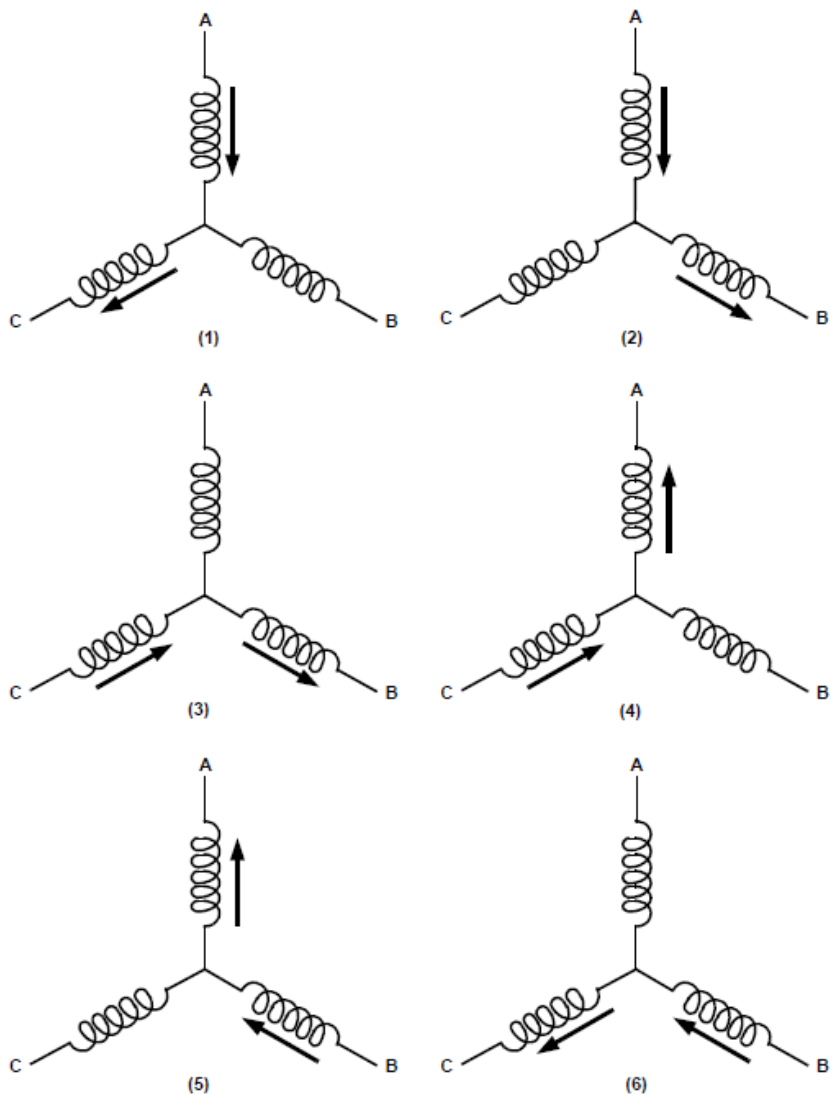
The simplest way to do this is by applying the PWM signal to either the high-side transistor or to the low-side transistor. Due to the re-

**Table 3.1:** Six-Step commutating sequence

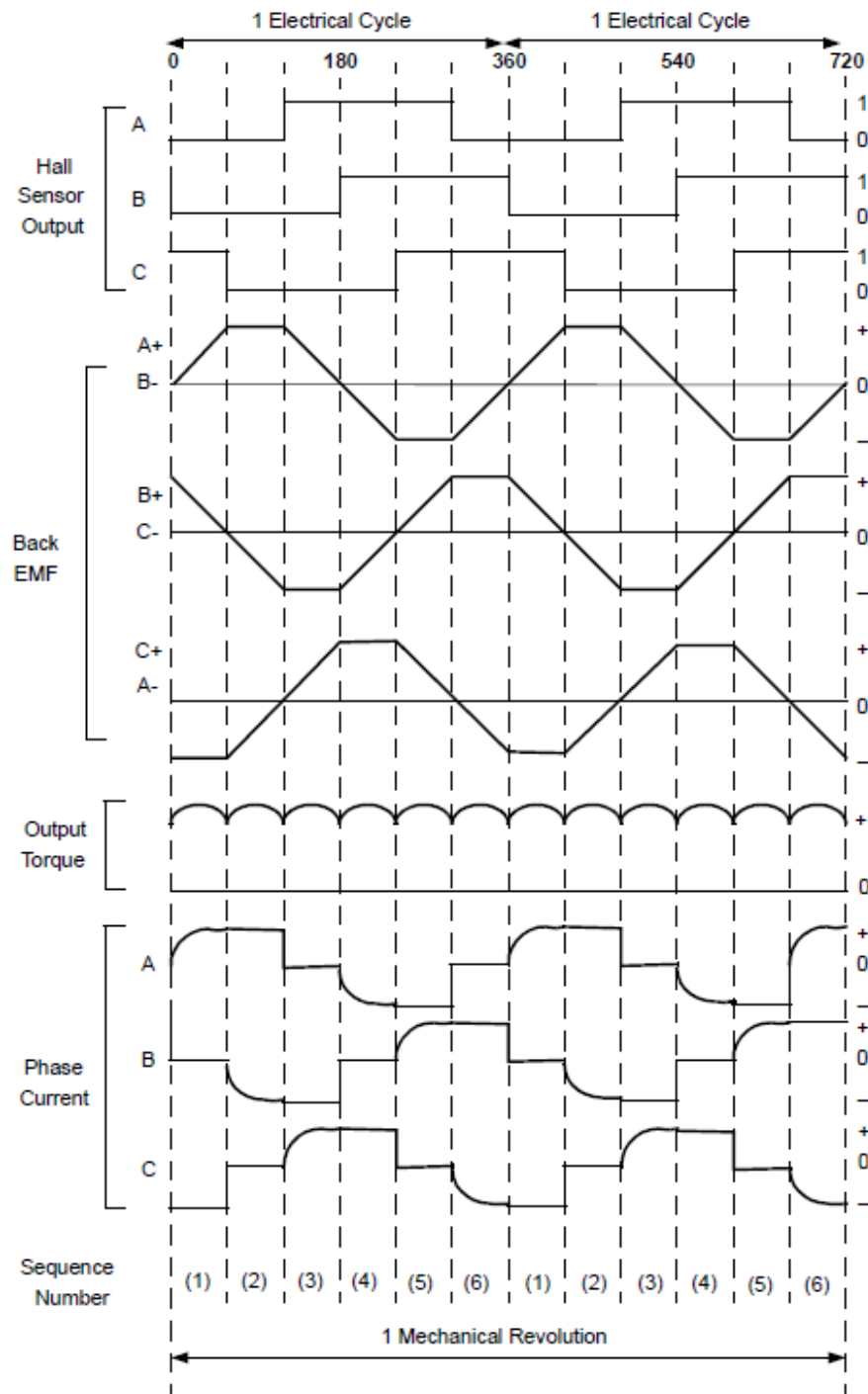
Clockwise Direction								
Sequence #	Hall Sensor Input			Active Gates		Phase Current		
	A	B	C	High Side	Low Side	A	B	C
1	1	0	0	$Q_B+$	$Q_A-$	DC-	DC+	Off
2	1	0	1	$Q_C+$	$Q_A-$	DC-	Off	DC+
3	0	0	1	$Q_C+$	$Q_B-$	Off	DC-	DC+
4	0	1	1	$Q_A+$	$Q_B-$	DC+	DC-	Off
5	0	1	0	$Q_A+$	$Q_C-$	DC+	Off	DC-
6	1	1	0	$Q_B+$	$Q_C-$	Off	DC+	DC-

Counter-Clockwise Direction								
Sequence #	Hall Sensor Input			Active Gates		Phase Current		
	A	B	C	High Side	Low Side	A	B	C
1	1	0	0	$Q_A+$	$Q_B-$	DC+	DC-	Off
2	1	0	1	$Q_A+$	$Q_C-$	DC+	Off	DC-
3	0	0	1	$Q_B+$	$Q_C-$	Off	DC+	DC-
4	0	1	1	$Q_B+$	$Q_A-$	DC-	DC+	Off
5	0	1	0	$Q_C+$	$Q_A-$	DC-	Off	DC+
6	1	1	0	$Q_C+$	$Q_B-$	Off	DC-	DC+



**Figure 3.18:** Current flowing through the coils of the PMAC motor in the 6-step commutation sequence



**Figure 3.19:** Six-Step commutation elements: Hall effect sensor signal, BEMF and output torque

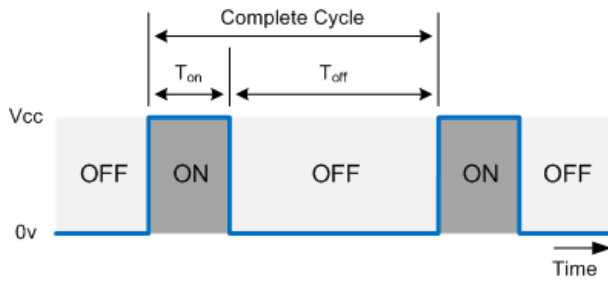


**Figure 3.20:** Pulse Width Modulation Signal

circulation diodes, the voltage in the windings energised would commutate from  $V_{DC}$  to 0V, as in a step-down voltage converter. A more complete approach to applying the six-step sequence with a lower voltage than  $V_{DC}$  to obtain a slower speed, would be to apply a complementary PWM signal to the low-side transistor on the same branch of the high-side transistor indicated on the sequence, while the low-side transistor indicated on the sequence stays enabled, as seen in Figure ???. This approach would allow us to brake the motor, enabling also the regenerative braking, since, by applying a complementary signal to the high-side transistor in the low-side transistor, we are allowing the flow of current not only from the power supply to the motor, but also from the motor to the power supply.

### 3.4.2 Sinusoidal Drive

The sinusoidal feeding for the **PMAC** motors is similar to feeding a three-phase induction motor, to which we need to provide a three-phase voltage in order to energise the windings and create a three-phase current. The difference in the power supply with the induction motor would be that the **PMAC** motor three-phase power supply needs to be synchronous with the rotor position. Therefore, after determining the absolute angular position of the rotor with any of the methods described in 3.3.2, we generate independent voltages for each phase using the three-phase inverter.

To generate these three independent voltage signals using the inverter, we can consider each one of the branches of the inverter as a voltage generator for each one of the phases. We can modulate a sinusoidal signal by using a **PWM** signal with a duty cycle  $D$  proportional to the amplitude of the sinusoidal signal, which can go from 0V up to  $V_{DC}$ :

$$D_{PWM} = \frac{v_a(\theta)}{V_{DC}} + 0.5 \quad (3.24)$$

By commutating the high-side transistor of the bridge with the **PWM** signal, and the low-side transistor with the complementary sig-

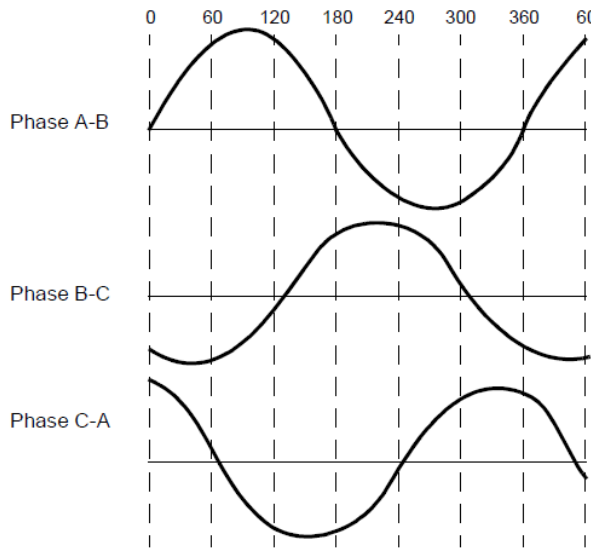


**Figure 3.21:** Sinusoidal BEMF

nal, in the three branches of the inverter, we generate a three-phase signal as the one seen in Figure 3.21.

It is important to recognize, from Equation 3.24, that if the voltage to be applied is larger than  $V_{DC}/2$ , the duty cycle  $D$  becomes larger than 1. Since a duty cycle larger than 1 doesn't make sense, the duty cycle will remain as 1 until the voltage applied becomes lower than  $V_{DC}/2$ , generating a trapezoidal waveform, which would have the same effect over the motor of the trapezoidal drive, losing the advantages of the sinusoidal drive.

This driving method is normally not used by itself, but it is applied in the Field Oriented Control (FOC) method, which will be explained at the end of this chapter.

### 3.5 ELECTRIC MOTOR CONTROL METHODS

As we have seen previously, there is a strong dependence between the rotating speed of the electric motor and the torque generated as a function of the voltage applied to its phases. This interaction can be seen in Figure 3.22. Due to this, and to the fact that there are many other external factors that might affect our system parameters, in order to obtain a desired speed or a desired torque, we can't just apply a previously calculated voltage that would give us those speed or torque values. Instead, we need to apply a control method in order to successfully reach a desired speed or a desired torque, by automatically comparing these quantities to the reference value that we want to achieve, and, in function of their difference, which is normally called "error signal"  $\varepsilon$ , change the driving signal of the inverter, using any of the previously seen driving methods.

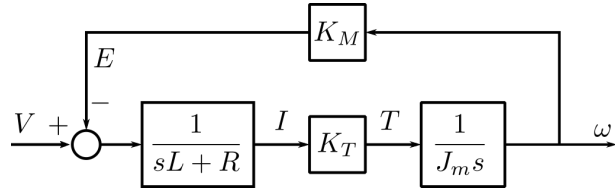


**Figure 3.22:** Coupling between mechanical and electrical dynamics on an electric motor

### 3.5.1 Speed Control

The speed control loop of an electric motor is achieved by means of applying a driving voltage into the motor coils, proportional to the error signal between a reference speed and the measured speed. This driving voltage is obtained by means of a Proportional-Integral (PI) controller. The PI controller creates a driving signal that is calculated by adding two signals. The first signal is the proportional error, which is equal to the error  $\varepsilon$  multiplied by a proportionality constant  $K_p$ . The second signal is the integral error, which is equal to the error  $\varepsilon$  multiplied by an integral constant  $K_i$  integrated over the time that the algorithm has been running (Figure 3.23).

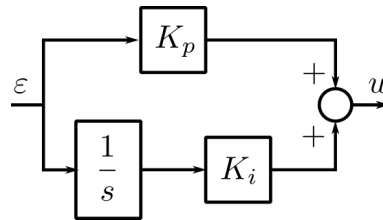


**Figure 3.23:** Blocks Diagram of a Proportional-Integral Controller

To apply the speed loop into the PMAC motors, we need to obtain the speed of rotation of the rotor. This can be easily done by deriving the position information provided by the Hall effect sensors embedded into the frame of the motor. After this, we calculate the error signal  $\varepsilon$ , pass it through the PI controller to generate a reference value that is applied to the inverter, which feeds the motor with the resulting voltage. As an example, we can see the speed control applied using the trapezoidal drive in Figure 3.24.

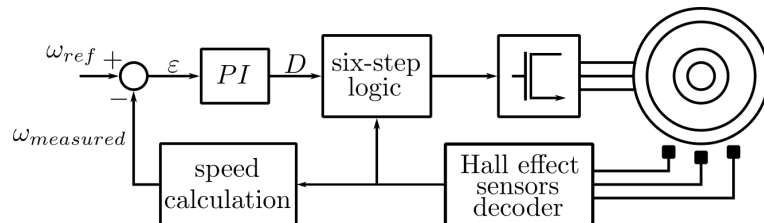


**Figure 3.24:** Speed Controller with Trapezoidal Drive

### 3.5.2 Torque Control

The torque control is based in Equation 3.11:

$$T = K_T I \quad (3.11)$$

where we can see that the torque applied by the motor is equal to the current flowing through its windings multiplied by the torque constant  $K_T$ . Therefore, we need to read the current flowing through the motor windings, using any of the methods mentioned in 3.3.3, to calculate the torque that the motor is applying by multiplying the current  $I_{measured}$  it by the torque constant  $K_T$ , and comparing it with the torque  $T_{ref}$  that we want the motor to apply. As we can see in Figure 3.25, the rest of the loop is similar to the speed loop.

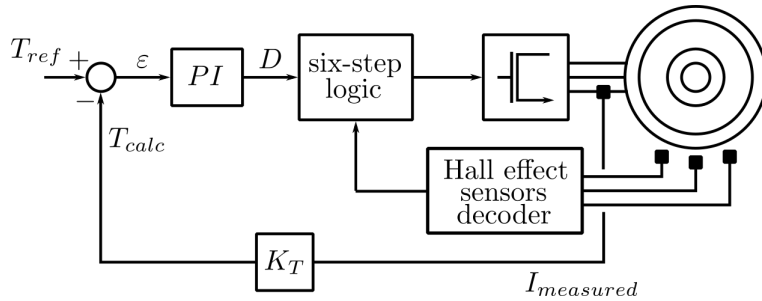


**Figure 3.25:** Torque Controller with Trapezoidal Drive

### 3.5.3 Field Oriented Control

The Field Oriented Control (FOC) or Vector Control, is technique that is applied with aims of controlling the current (and therefore the torque) of the PMAC motor in the same way that the current of a DC motor is controlled. This is done because the DC motor has the advantage that, in any case, the magnetic field of the rotor is always synchronized with the magnetic field of the permanent magnets attached to its stator due to the mechanical commutators, which makes it very easy to control. Instead, the PMAC motors must be synchronized by means of applying different driving algorithms depending on the rotor angular position, as mentioned before in this chapter. To achieve this, we need to make variable transformations to the voltage and current values of the system in order to control the system using only two variables: the quadrature current  $I_q$  and the direct current  $I_d$ .

To achieve the FOC we start by transforming the current signals that we acquire from the current sensors using the Clarke Transformation, which converts the three current phasors of the motor into two equivalent currents based on the  $\alpha$  and  $\beta$  axis:

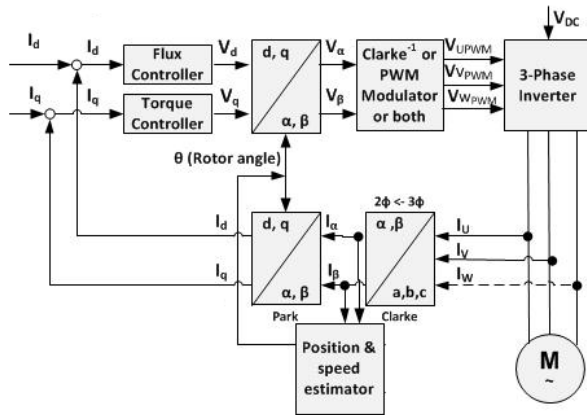


**Figure 3.26:** Field Oriented Control Blocks Diagram

$$\begin{bmatrix} i_\alpha \\ i_\beta \end{bmatrix} = \frac{2}{3} \begin{bmatrix} 1 & -\frac{1}{2} & -\frac{1}{2} \\ 0 & \frac{\sqrt{3}}{2} & -\frac{\sqrt{3}}{2} \end{bmatrix} \begin{bmatrix} i_a \\ i_b \\ i_c \end{bmatrix}$$

After this, in order to have two currents that don't change in function of the angular position of the rotor \$\theta\$, we apply the Park Transformation, which converts the currents \$i\_\alpha\$ and \$i\_\beta\$ into two currents that are based into an axis that rotates with the same angle as the rotor:

$$\begin{bmatrix} I_d \\ I_q \end{bmatrix} = \begin{bmatrix} \cos \theta & \sin \theta \\ -\sin \theta & \cos \theta \end{bmatrix} \begin{bmatrix} i_\alpha \\ i_\beta \end{bmatrix}$$

We can compare these two currents, \$I\_q\$ and \$I\_d\$, with the reference currents \$I\_{q,ref}\$ and \$I\_{d,ref}\$, generating error signals \$\varepsilon\_q\$ and \$\varepsilon\_d\$ that pass through PI controllers in order to generate two voltage values \$V\_q\$ and \$V\_d\$, which can be transformed into sinusoidal voltages \$v\_a\$, \$v\_b\$ and \$v\_c\$.

To obtain these voltage values, we apply the Inverse Park transform to the quadrature and direct voltages \$V\_q\$ and \$V\_d\$:

$$\begin{bmatrix} v_\alpha \\ v_\beta \end{bmatrix} = \begin{bmatrix} \cos \theta & -\sin \theta \\ \sin \theta & \cos \theta \end{bmatrix} \begin{bmatrix} V_d \\ V_q \end{bmatrix}$$

and then, the Inverse Clark Transform:

$$\begin{bmatrix} v_a \\ v_b \\ v_c \end{bmatrix} = \frac{3}{2} \begin{bmatrix} \frac{2}{3} & 0 \\ -\frac{1}{3} & \frac{\sqrt{3}}{3} \\ -\frac{1}{3} & -\frac{\sqrt{3}}{3} \end{bmatrix} \begin{bmatrix} v_\alpha \\ v_\beta \end{bmatrix}$$

Finally, we apply these \$v\_a\$, \$v\_b\$ and \$v\_c\$ values and apply them to the inverter applying the sinusoidal drive method explained in 3.4.2.

### 3.5.4 Speed Control with Field Oriented Control

Since by applying the FOC method to PMAC motors we can achieve a good current control, we can therefore control the torque produced by the motor with the same performance. Due to this, the best option to control the speed of a PMAC motor is to close a speed loop around the FOC loop as the one shown in Figure 3.27.

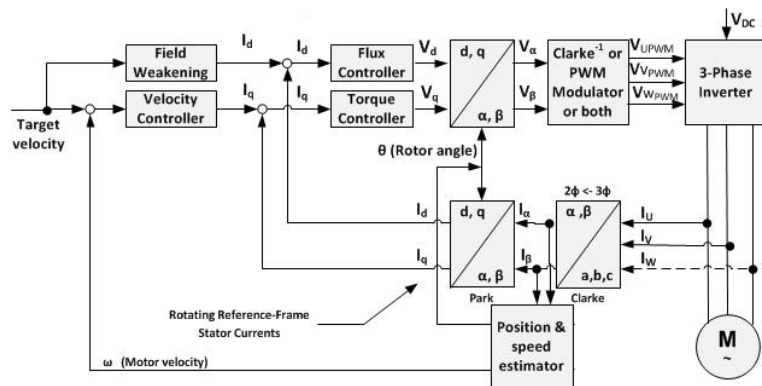


**Figure 3.27:** Field Oriented Control Applied in Speed Control



# 4

## STUDY CASE

---

This thesis was proposed as part of a robotic agriculture project which consists in the development of a mobile manipulator for agricultural applications called ROBI'. In this chapter we will explain the main characteristics of the project, focusing in the electronic architecture and in the systems that should be controlled by the motor driver developed in this thesis. The information for this chapter was obtained from Bascetta, Baur, and Gruosso "ROBI': A Prototype Mobile Manipulator for Agricultural Applications" 2017 and from Bascetta, Baur, and Gruosso "Electrical Unmanned Vehicle Architecture for precision farming applications" 2017.

### 4.1 ROBI

ROBI' is a mobile manipulator for agricultural applications. The development of this project has the objective of becoming a platform for research, development and testing of different perception and control algorithms. The robot was designed following low-cost, low-weight, simplicity, flexibility and modularity requirements, in order to allow an easy implementation of the work developed as part of this project.



**Figure 4.1:** ROBI' Basic Configuration

**Table 4.1:** HUB10GL in-wheel motor main characteristics

Motor mass	3.5 kg
Motor and tire mass	5.7 kg
Tire diameter	254 mm
Power	500 W
Voltage	36 V
Maximum speed	1350 RPM
Phase-to-phase resistance	160 mΩ
Phase-to-phase inductance	0.76 mH
Pole Pairs	10
$K_E$	0.36 V/(rad/s)
$K_T$	0.4506 Nm/A

## 4.2 IN-WHEEL MOTORS

One of the most important components of ROBI' for this thesis is the in-wheel motor system used as motor drive. As mentioned in the introduction, in-wheel motors have the advantage that there is no need for an external power transmission mechanism, due to the fact that the motor is embedded into the wheel. This also reduces the space needed for the motor drive system, as well as the weight of the robot, increasing the payload capacity of the electric motor.

It is also interesting to mention that this configuration of the drive system allows the control of each one of the wheels of the robot independently, which allows the implementation of different control methods for this robot, like skid steering, which relies on the slip effect of the wheels in the terrain and requires a good control of the torque and the speed of each one of the motors.

The in-wheel motor installed in the robot is a **PMSM** motor and its main characteristics are mentioned in Table 4.1.

In order to take advantage of the sinusoidal distribution of the windings of this motor, an absolute angular position sensor was installed in the drive system in order to be able to apply a **FOC** loop. The sensor was attached to the wheel by means of a toothed pulley system in order to keep it away from the ground.

The angular position sensor used is an Orbis encoder, manufactured by RLS. As mentioned in 3.3.2, this is a magnetic encoder which works by reading the orientation of the magnetic field of a permanent magnet attached to a shaft. The encoder has a resolution of 14 bits with a sensitivity of  $\pm 0.3^\circ$  and transmits the angular position information through a modified Serial Peripheral Interface (**SPI**) called Synchronous Serial Interface (**SSI**), which sends the 14 bits in **SPI** slave write-only mode through a RS422 transceiver.



**Figure 4.2:** Encoder transmission configuration

**Table 4.2:** Battery main characteristics

Manufacturer	FIAM
Model	FGC22703
Type	Sealed lead acid
Voltage	12 V
Capacity	27 Ah

In this case, the shaft is not directly the shaft of the rotor, but it's the shaft of the pulley system. This transmission system has a 4.6 size ratio due to the space constraints of the system. As mentioned in [3.3.2](#), this motor includes three Hall effect sensors, even if it's a [PMSM](#) motor.

#### 4.3 POWER ARCHITECTURE

Another important aspect for the development of this work is the power supply. In the case of ROBI', the power supply consists on three 12V lead acid deep-cycle batteries connected in series to provide 36V to the different components of the robot.

#### 4.4 ELECTRONIC ARCHITECTURE

It is important to understand the expected electronic architecture in order to consider the peripherals that the microcontroller has to include to communicate with the rest of the systems inside the robot.

The electronic architecture of ROBI' was designed to be similar to an automotive Electronic Control Unit ([ECU](#)) based system. In this architectures, all the [ECUs](#) interact with each other through a communication bus called Controller Area Network ([CAN](#)).

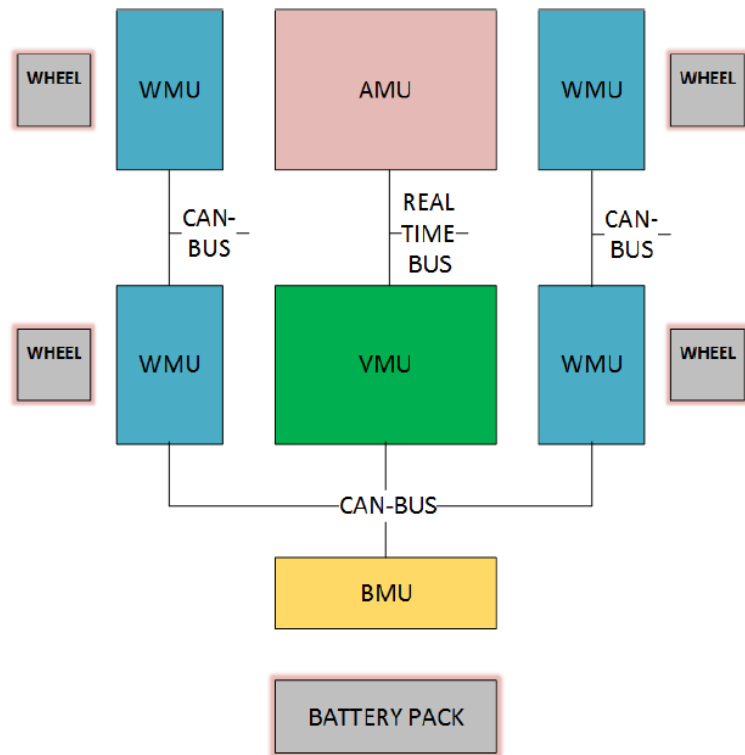


**Figure 4.3:** ECUs architecture: functional block diagram

As it can be seen in Figure 4.3, the ECUs network consists on four units: Wheel Management Unit (**WMU**), Battery Management Unit (**BMU**), Vehicle Management Unit (**VMU**) and Arm Management Unit (**AMU**). The one that is being developed here is the **WMU**, and it will be described in the following chapters.

# 5

## PROJECT DEVELOPMENT

---

(...)

### 5.1 HYPOTHESIS

(...)

### 5.2 VESC BOARD

The electric drive on which the motor controller is based is an open architecture project developed by the Swedish engineer Benjamin Veder called VESC, which consists in the hardware design of a [PCB](#) and the source code used to drive a [BLDC](#) motor.

The VESC board was conceived and designed to be used in electric skateboards with the intention to create one of the best electronic speed controllers available. Since it was planned to be used in a skateboard, it has a small form-factor and it can be used for different applications with similar power demand. The hardware can also be modified by changing specific components to drive motors with higher power demand or by modifying the [PCB](#) following the schematic design.

The board consists of the following blocks, which will be explained in detail in this chapter:

1. Power supply input
2. Power MOSFETs three-phase inverter
3. MOSFET driver
4. Microcontroller unit
5. Peripherals
  - a) Temperature sensors
    - i. Motor temperature sensor
    - ii. Board temperature sensor
  - b) Hall effect sensors
  - c) RC Servomotor Output

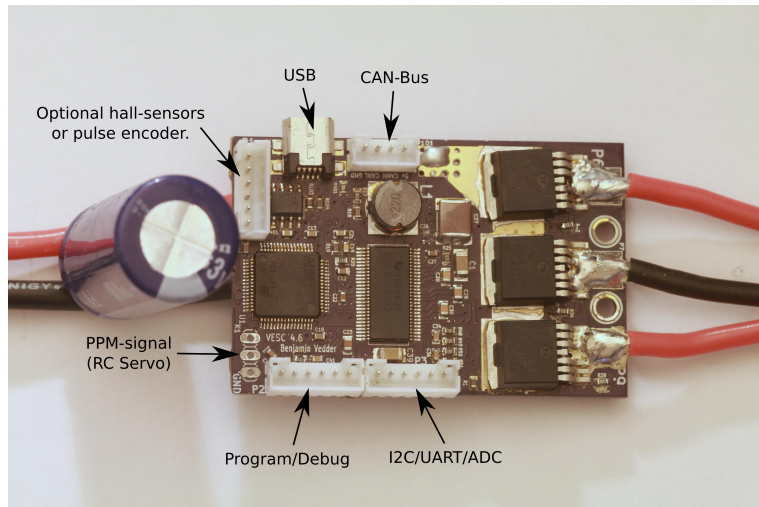


**Figure 5.1:** Front Side of the VESC Board. The three wires at soldered at the right edge of the board are connected to the three phases of the brushless motor.

d) Debug LEDs

## 6. Communication interfaces

- a) USB
- b) CAN
- c) USART
- d) SPI
- e) I<sub>2</sub>C

### 5.2.1 Power Supply Input

The power is supplied into the board by means of soldering 2 wires into large pads placed closely to the three-phase inverter nodes *V\_SUPPLY* and *GND*. *V\_SUPPLY* and *GND* are the positive and negative nodes of the power supply source respectively. The power is supplied from a power regulator for static applications or from a battery for mobile applications, like in the case of ROBI'. It is also specified that there should be a decoupling capacitor connected in parallel to the power supply port.

#### 5.2.1.1 Power Supply Range

The voltage range of the VESC board is defined by the [MOSFET](#) driver integrated circuit DRV8302, which specifies an operating supply voltage range from 8V to 60V, but allows a maximum voltage supply up to 65V [??](#). All the other components of the board, mainly capacitors and power [MOSFETs](#), must be selected according to this voltage range.

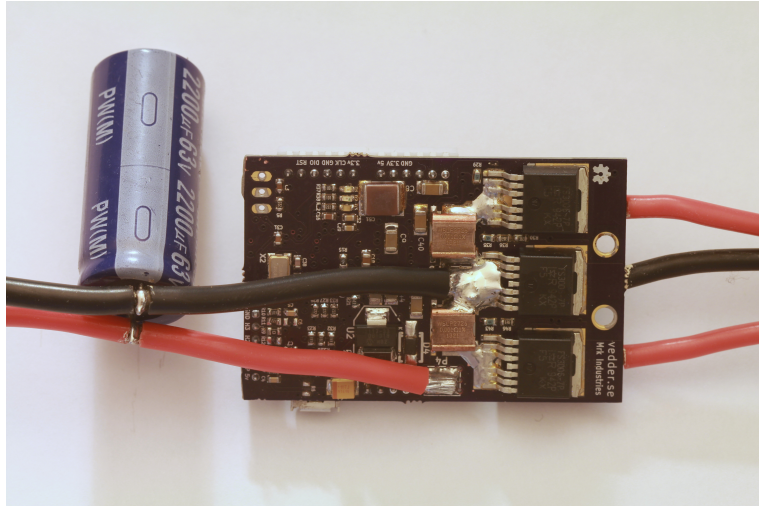


**Figure 5.2:** Back Side of the VESC board. The red and black wires are the power supply input  $V\_SUPPLY$  and  $GND$  respectively.

The current range of the board is limited by the [MOSFETs](#) current limit and by the width of the traces in the [PCB](#). This maximum values will be addressed later in the section dedicated to the power [MOSFETs](#) used in the board.

### 5.2.1.2 Bulk Electrolytic Capacitor

It is important to place a bulk capacitance with an appropriate capacitance value and voltage range in parallel to the input of the power supply of a motor drive system. The main objective of a bulk capacitance is to control the voltage deviation at the input of a system when the converter is responding to an output load transient, meaning that if there is a load increase and the power supply is not able to provide the current instantaneously for the motor, the current must be provided by the bulk capacitor. The higher the capacitance at the input of the system, the lower the deviation at the load, but this comes at a cost of price and space, since the capacitance value of a capacitor is proportional to the size of its parallel plates. The value of the input bulk capacitor is determined mainly by the following factors:

1. The largest amount of current required by the motor
  2. The capacitance of the power supply and its ability to source current
  3. The parasitic inductance between the power supply and the motor
  4. The acceptable voltage ripple
  5. The type of motor

The datasheet of a motor driver should generally provide a recommended value for the bulk capacitor, but it is necessary to calculate and test the value to determine if it's appropriate. The voltage rating of a bulk capacitor must be higher than the value of the power supply to provide a margin for cases in which the motor transfers energy to the supply, which would increase its voltage and would damage a capacitor with a smaller value than the resulting voltage.

The magnitude of the input transient is calculated as following:

$$\Delta I_{in} = \frac{V_{out}}{V_{in}\eta} \cdot \Delta I_{out} \quad (5.1)$$

where  $\eta$  is efficiency,  $\Delta I_{out}$  is the output transient current,  $\Delta I_{in}$  is the input transient current,  $V_{out}$  is the nominal output voltage and  $V_{in}$  is the nominal input voltage. After determining the input transient, we can calculate the capacitance value by using the following formula:

$$C = \frac{1.21 \cdot I_{tr}^2 \cdot L}{\Delta V^2} \quad (5.2)$$

Since there is no filtering inductance in the system, we can consider a stray inductance of 50 nH in the calculation. If we consider a transient current  $I_{tr}$  equal to the rated current of the in-wheel motor, 14A approximately, and a voltage ripple of 100mV, we obtain a capacitance value of 1185.8 $\mu$ F for the bulk capacitance. By looking for commercially available capacitor values, we can increase the value of the capacitor to 2200uF and, considering the maximum input voltage value of the motors, we need double that value and define a voltage range of 70V, which is a commercially available value for a capacitor.

The voltage of the capacitor is chosen double of the rated voltage of the motor because it is possible that, when the motor enters a braking mode, the energised coils apply a voltage equal to the **BEMF** and the voltage bus  $V_{DC}$  increases up to  $2 \cdot V_{DC}$ .

It is important to note that since the value of this capacitance is large, also its size will be large, therefore it's important to consider its dimensions to setup a mechanically stable position for such capacitance with aims of avoiding hardware malfunction.

### 5.2.1.3 Power Supply Wiring

The strategy of soldering the wires directly to the pads in the **PCB** helps reduce the size and price of the board since it avoids the use of large power traces in that would be needed if a regular receptacle connector was to be used.

Anyway, the practice of soldering a wire directly to a **PCB** is discouraged mainly in circuits that will be mounted in a system designed to be in movement (i.e. automotive or aerospace applications) because

the wire used in these applications is made of delicate copper strands which can break easily with movement of the board or of the wires and cause a short circuit or a loose contact, both of which might lead to catastrophic failures , so there is a risk in this board since it will be mounted in systems that will be in constant movement. Since this board was designed this way to reduce space consumption, the trade-off between safety and size was balanced into the size constraints, therefore some cautions must be taken to avoid problems, mainly because these wires carry a considerable amount of current and they pass over many components of the board as seen in Figure 5.2.

The first consideration to be made is the wire gauge and insulation type. The wire gauge is a measurement of the wire diameter, which determines the amount of electric current that a wire can safely carry, as well as its electrical resistance and weight. Since the wire has an implicit resistance depending on its diameter as stated by Pouillet's Law:

$$R = \frac{\rho L}{A} \quad (5.3)$$

where  $\rho$  is the electrical resistivity of the material,  $L$  is the length of the wire and  $A$  is the cross-sectional area of the wire, there is also a voltage drop in the transmission line depending on the current flowing through the wire. This voltage drop can be neglected or not depending on the length of the wire being used, which defines 2 types of wiring: chassis wiring and transmission line wiring. For this board, it is suggested to use short wires to avoid a large voltage drop and to ease the handling of such wire until it reaches the output of the enclosure that will protect the circuit. In either case, the wire can be considered as chassis wiring since a transmission line wiring is considered for wires larger than 2 meters.

The second consideration regarding the wire selection is the insulation material. Since the current passing through the copper also implies power consumption due to the resistance of the copper, there is heat transfer from the wire to its surroundings. To protect the copper strands from its surroundings and vice versa, wires are covered by an insulating material, which has low thermal and electrical conductivity.

Since the heat exchange calculation of the wire would require many assumptions, it's a normal practice to select the type of wire using tables that consider the temperature rise in the wire according to different currents and lengths. In the case of the PMSM motor used in ROBI', the maximum steady state current would be approximately 14A, therefore we can use a table of wire gauges and currents under (...)

### 5.2.2 Power MOSFET Three-Phase Inverter

The three-phase inverter used in the VESC board is based on the power [MOSFET](#) IRFS7530-7PPbF, manufactured by the semiconductor company International Rectifier.

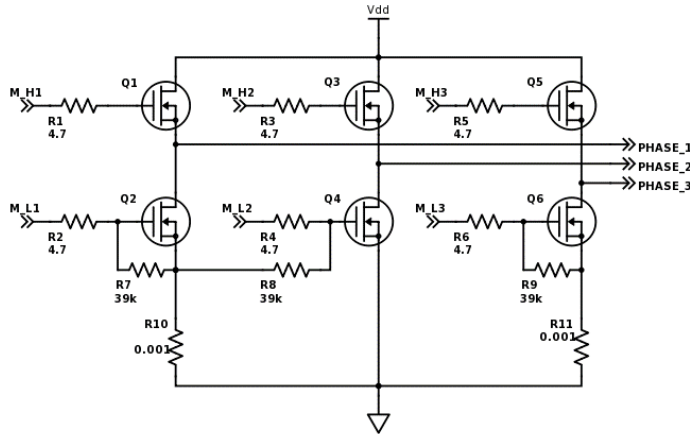


**Figure 5.3:** Three-phase inverter implemented using power MOSFETs.

This [MOSFET](#) is based on the HEXFET Power [MOSFET](#) technology, which is a Vertical Double-diffused MOS transistor (VDMOS) with hexagonal elementary cells in parallel which maximizes the  $W/L$  ratio of the transistor, reducing its on-resistance  $R_{DS(ON)}$ .

	<b>V<sub>DSS</sub></b>	<b>60V</b>
	<b>R<sub>DS(on)</sub> typ.</b>	<b>1.15mΩ</b>
	<b>max</b>	<b>1.4mΩ</b>
	<b>I<sub>D</sub> (Silicon Limited)</b>	<b>338A①</b>
	<b>I<sub>D</sub> (Package Limited)</b>	<b>240A</b>

**Figure 5.4:** ...

#### 5.2.2.1 Switching Times

#### 5.2.3 MOSFET Driver

The central component in the VESC board around which the rest of the circuit was designed is the integrated circuit *DRV8302*, a brushless motor inverter manufactured by Texas Instruments.

The *DRV8302* provides three half bridge drivers capable of driving two N-channel MOSFETs each. (...)

The device supports up to 1.7-A source and 2.3-A peak current capability. (...)

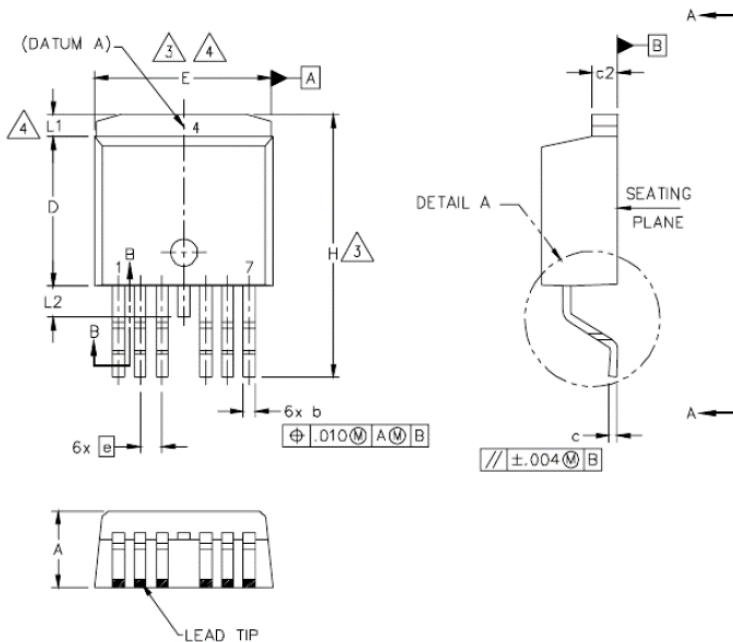


**Figure 5.5:** ...

The DRV8302 can operate off of a single power supply with a wide range from 8-V to 60-V. (...)

It uses a bootstrap gate driver architecture with trickle charge circuitry to support 100 duty cycle. (...)

The DRV8302 uses automatic hand shaking when the high side or low side MOSFET is switching to prevent current shoot through. (...)

Integrated VDS sensing of the high and low side MOSFETs is used to protect the external power stage against overcurrent conditions. (...)

The DRV8303 includes two current shunt amplifiers for accurate current measurement. The amplifiers support bi-directional current sensing and provide and adjustable output offset up to 3 V. (...)

The DRV8302 also includes an integrated switching mode buck converter with adjustable output and switching frequency. The buck converter can provide up to 1.5 A to support MCU or additional system power needs. (...)

A hardware interface allows for configuring various device parameters including dead time, overcurrent, PWM mode, and amplifier settings. Error conditions are reported through the nFAULT and nOCTW pins. 3.3-V and 5-V Interface Support. (...)

#### 5.2.4 Microcontroller Unit

The processor for which this board was designed is the STM32F405rg: a 64-pin IC microcontroller of the STMicroelectronics family of 32-bit devices with an ARM Cortex-M4 CPU and a core operating frequency up to 168 MHz. The Cortex-M4 core features a Floating Point

Unit ([FPU](#)) single precision which supports all ARM single-precision data-processing instructions and data types. It also implements a full set of Digital Signal Processor ([DSP](#)) instructions, which makes it ideal for the signal processing required to drive [PMAC](#) motors. This microcontroller also includes three 12-bit [ADCs](#) and supports USART, I<sub>2</sub>C, SPI, USB and CAN communication interfaces, improving the versatility of the VESC board. The memory of the microcontroller consists in 1024 kB of Flash memory and 192 kB of SRAM memory.

### 5.2.5 *PCB Layout*

(...)

## 5.3 MEASUREMENT BOARD

(...)

### 5.3.1 *Voltage Measurement*

(...)

### 5.3.2 *Current Measurement*

(...)

### 5.3.3 *Data acquisition*

(...)

## 5.4 ANGULAR POSITION SENSOR

(...)

## 5.5 MIOSIX

(...)

## 5.6 TEST SETUP

(...)

### 5.6.1 Robi Setup

(...)

#### 5.6.1.1 Marelli Generator as Load

(...)

## 5.7 ALGORITHMS IMPLEMENTATION

(...)

### 5.7.1 6-Step Drive Implementation

(...)

### 5.7.2 Field Oriented Control Implementation

(...)



# 6

## RESULTS

---

(...)

Lorem ipsum dolor sit amet, consectetuer adipiscing elit. Ut purus elit, vestibulum ut, placerat ac, adipiscing vitae, felis. Curabitur dictum gravida mauris. Nam arcu libero, nonummy eget, consectetuer id, vulputate a, magna. Donec vehicula augue eu neque. Pellentesque habitant morbi tristique senectus et netus et malesuada fames ac turpis egestas. Mauris ut leo. Cras viverra metus rhoncus sem. Nulla et lectus vestibulum urna fringilla ultrices. Phasellus eu tellus sit amet tortor gravida placerat. Integer sapien est, iaculis in, pretium quis, viverra ac, nunc. Praesent eget sem vel leo ultrices bibendum. Aenean faucibus. Morbi dolor nulla, malesuada eu, pulvinar at, mollis ac, nulla. Curabitur auctor semper nulla. Donec varius orci eget risus. Duis nibh mi, congue eu, accumsan eleifend, sagittis quis, diam. Duis eget orci sit amet orci dignissim rutrum.

### 6.1 BLDC

(...)

Nam dui ligula, fringilla a, euismod sodales, sollicitudin vel, wisi. Morbi auctor lorem non justo. Nam lacus libero, pretium at, lobortis vitae, ultricies et, tellus. Donec aliquet, tortor sed accumsan bibendum, erat ligula aliquet magna, vitae ornare odio metus a mi. Morbi ac orci et nisl hendrerit mollis. Suspendisse ut massa. Cras nec ante. Pellentesque a nulla. Cum sociis natoque penatibus et magnis dis parturient montes, nascetur ridiculus mus. Aliquam tincidunt urna. Nulla ullamcorper vestibulum turpis. Pellentesque cursus luctus mauris.

#### 6.1.1 *Voltage Waveforms*

(...)

Nulla malesuada porttitor diam. Donec felis erat, congue non, volutpat at, tincidunt tristique, libero. Vivamus viverra fermentum felis. Donec nonummy pellentesque ante. Phasellus adipiscing semper elit. Proin fermentum massa ac quam. Sed diam turpis, molestie vitae, placerat a, molestie nec, leo. Maecenas lacinia. Nam ipsum ligula, eleifend at, accumsan nec, suscipit a, ipsum. Morbi blandit ligula

feugiat magna. Nunc eleifend consequat lorem. Sed lacinia nulla vitae enim. Pellentesque tincidunt purus vel magna. Integer non enim. Praesent euismod nunc eu purus. Donec bibendum quam in tellus. Nullam cursus pulvinar lectus. Donec et mi. Nam vulputate metus eu enim. Vestibulum pellentesque felis eu massa.

#### 6.1.2 Current Waveforms

(...)

Quisque ullamcorper placerat ipsum. Cras nibh. Morbi vel justo vitae lacus tincidunt ultrices. Lorem ipsum dolor sit amet, consectetur adipiscing elit. In hac habitasse platea dictumst. Integer tempus convallis augue. Etiam facilisis. Nunc elementum fermentum wisi. Aenean placerat. Ut imperdiet, enim sed gravida sollicitudin, felis odio placerat quam, ac pulvinar elit purus eget enim. Nunc vitae tortor. Proin tempus nibh sit amet nisl. Vivamus quis tortor vitae risus porta vehicula.

#### 6.1.3 Voltage Control Plots

(...)

Fusce mauris. Vestibulum luctus nibh at lectus. Sed bibendum, nulla a faucibus semper, leo velit ultricies tellus, ac venenatis arcu wisi vel nisl. Vestibulum diam. Aliquam pellentesque, augue quis sagittis posuere, turpis lacus congue quam, in hendrerit risus eros eget felis. Maecenas eget erat in sapien mattis porttitor. Vestibulum porttitor. Nulla facilisi. Sed a turpis eu lacus commodo facilisis. Morbi fringilla, wisi in dignissim interdum, justo lectus sagittis dui, et vehicula libero dui cursus dui. Mauris tempor ligula sed lacus. Duis cursus enim ut augue. Cras ac magna. Cras nulla. Nulla egestas. Curabitur a leo. Quisque egestas wisi eget nunc. Nam feugiat lacus vel est. Curabitur consectetur.

#### 6.1.4 Current Control Plots

(...)

Suspendisse vel felis. Ut lorem lorem, interdum eu, tincidunt sit amet, laoreet vitae, arcu. Aenean faucibus pede eu ante. Praesent enim elit, rutrum at, molestie non, nonummy vel, nisl. Ut lectus eros, malesuada sit amet, fermentum eu, sodales cursus, magna. Donec eu purus. Quisque vehicula, urna sed ultricies auctor, pede lorem egestas dui, et convallis elit erat sed nulla. Donec luctus. Curabitur et nunc. Aliquam dolor odio, commodo pretium, ultricies non, pharetra

in, velit. Integer arcu est, nonummy in, fermentum faucibus, egestas vel, odio.

## 6.2 PMSM

(...)

Sed commodo posuere pede. Mauris ut est. Ut quis purus. Sed ac odio. Sed vehicula hendrerit sem. Duis non odio. Morbi ut dui. Sed accumsan risus eget odio. In hac habitasse platea dictumst. Pellentesque non elit. Fusce sed justo eu urna porta tincidunt. Mauris felis odio, sollicitudin sed, volutpat a, ornare ac, erat. Morbi quis dolor. Donec pellentesque, erat ac sagittis semper, nunc dui lobortis purus, quis congue purus metus ultricies tellus. Proin et quam. Class aptent taciti sociosqu ad litora torquent per conubia nostra, per inceptos hymenaeos. Praesent sapien turpis, fermentum vel, eleifend faucibus, vehicula eu, lacus.

### 6.2.1 *Voltage Waveforms*

(...)

Pellentesque habitant morbi tristique senectus et netus et malesuada fames ac turpis egestas. Donec odio elit, dictum in, hendrerit sit amet, egestas sed, leo. Praesent feugiat sapien aliquet odio. Integer vitae justo. Aliquam vestibulum fringilla lorem. Sed neque lectus, consectetur at, consectetur sed, eleifend ac, lectus. Nulla facilisi. Pellentesque eget lectus. Proin eu metus. Sed porttitor. In hac habitasse platea dictumst. Suspendisse eu lectus. Ut mi mi, lacinia sit amet, placerat et, mollis vitae, dui. Sed ante tellus, tristique ut, iaculis eu, malesuada ac, dui. Mauris nibh leo, facilisis non, adipiscing quis, ultrices a, dui.

### 6.2.2 *Current Waveforms*

(...)

Morbi luctus, wisi viverra faucibus pretium, nibh est placerat odio, nec commodo wisi enim eget quam. Quisque libero justo, consectetur a, feugiat vitae, porttitor eu, libero. Suspendisse sed mauris vitae elit sollicitudin malesuada. Maecenas ultricies eros sit amet ante. Ut venenatis velit. Maecenas sed mi eget dui varius euismod. Phasellus aliquet volutpat odio. Vestibulum ante ipsum primis in faucibus orci luctus et ultrices posuere cubilia Curae; Pellentesque sit amet pede ac sem eleifend consectetur. Nullam elementum, urna vel imperdiet sodales, elit ipsum pharetra ligula, ac pretium ante justo a nulla. Cur-

abitur tristique arcu eu metus. Vestibulum lectus. Proin mauris. Proin eu nunc eu urna hendrerit faucibus. Aliquam auctor, pede consequat laoreet varius, eros tellus scelerisque quam, pellentesque hendrerit ipsum dolor sed augue. Nulla nec lacus.

#### 6.2.3 *Voltage Control Plots*

(...)

Suspendisse vitae elit. Aliquam arcu neque, ornare in, ullamcorper quis, commodo eu, libero. Fusce sagittis erat at erat tristique mollis. Maecenas sapien libero, molestie et, lobortis in, sodales eget, dui. Morbi ultrices rutrum lorem. Nam elementum ullamcorper leo. Morbi dui. Aliquam sagittis. Nunc placerat. Pellentesque tristique sodales est. Maecenas imperdiet lacinia velit. Cras non urna. Morbi eros pede, suscipit ac, varius vel, egestas non, eros. Praesent malesuada, diam id pretium elementum, eros sem dictum tortor, vel consectetur odio sem sed wisi.

#### 6.2.4 *Current Control Plots*

(...)

## CONCLUSION

---

(...)

Lorem ipsum dolor sit amet, consectetuer adipiscing elit. Ut purus elit, vestibulum ut, placerat ac, adipiscing vitae, felis. Curabitur dictum gravida mauris. Nam arcu libero, nonummy eget, consectetuer id, vulputate a, magna. Donec vehicula augue eu neque. Pellentesque habitant morbi tristique senectus et netus et malesuada fames ac turpis egestas. Mauris ut leo. Cras viverra metus rhoncus sem. Nulla et lectus vestibulum urna fringilla ultrices. Phasellus eu tellus sit amet tortor gravida placerat. Integer sapien est, iaculis in, pretium quis, viverra ac, nunc. Praesent eget sem vel leo ultrices bibendum. Aenean faucibus. Morbi dolor nulla, malesuada eu, pulvinar at, mollis ac, nulla. Curabitur auctor semper nulla. Donec varius orci eget risus. Duis nibh mi, congue eu, accumsan eleifend, sagittis quis, diam. Duis eget orci sit amet orci dignissim rutrum.

### 7.1 BLA BLA BLA

(...)

Nam dui ligula, fringilla a, euismod sodales, sollicitudin vel, wisi. Morbi auctor lorem non justo. Nam lacus libero, pretium at, lobortis vitae, ultricies et, tellus. Donec aliquet, tortor sed accumsan bibendum, erat ligula aliquet magna, vitae ornare odio metus a mi. Morbi ac orci et nisl hendrerit mollis. Suspendisse ut massa. Cras nec ante. Pellentesque a nulla. Cum sociis natoque penatibus et magnis dis parturient montes, nascetur ridiculus mus. Aliquam tincidunt urna. Nulla ullamcorper vestibulum turpis. Pellentesque cursus luctus mauris.

### 7.2 FUTURE WORK

(...)

Nulla malesuada porttitor diam. Donec felis erat, congue non, volutpat at, tincidunt tristique, libero. Vivamus viverra fermentum felis. Donec nonummy pellentesque ante. Phasellus adipiscing semper elit. Proin fermentum massa ac quam. Sed diam turpis, molestie vitae, placerat a, molestie nec, leo. Maecenas lacinia. Nam ipsum ligula, eleifend at, accumsan nec, suscipit a, ipsum. Morbi blandit ligula

feugiat magna. Nunc eleifend consequat lorem. Sed lacinia nulla vitae enim. Pellentesque tincidunt purus vel magna. Integer non enim. Praesent euismod nunc eu purus. Donec bibendum quam in tellus. Nullam cursus pulvinar lectus. Donec et mi. Nam vulputate metus eu enim. Vestibulum pellentesque felis eu massa.

## BIBLIOGRAPHY

---

- Bascetta, Luca, Marco Baur, and Giambattista Gruosso (2017a). "Electrical Unmanned Vehicle Architecture for precision farming applications." In: (cit. on p. 39).
- (2017b). "ROBI': A Prototype Mobile Manipulator for Agricultural Applications." In: *MDPI Electronics* (cit. on pp. 2, 6, 39).
- Bose, B. K., T. M. Jahns, R. D. Lorenz, G. Pfaff, P. Pillay, M. H. Rashid, T. Sebastian, and G. R. Slemon (1989). *Performance and Design of Permanent Magnet AC Motor Drives*. IEEE (cit. on p. 9).
- Doppelbauer, Martin (2012). *The Invention of the Electric Motor*. URL: <https://www.eti.kit.edu/english/1376.php> (visited on 02/28/2012) (cit. on p. 1).
- Electrical Motors Basic Components (2012). URL: <http://www.electrical-knowhow.com/2012/05/electrical-motors-basic-components.html> (visited on 05/01/2012) (cit. on p. 10).
- Ghioni, Massimo. *Introduction to Electrical Drives*. URL: <ftp://ftp.elet.polimi.it/users/Massimo.Ghioni/Power%20Electronics%20/Motor%20control/motor%20control%20overview/INTRODUCTION%20TO%20ELECTRICAL%20DRIVES.pdf> (cit. on p. 20).
- (2016). *Lecture notes in Power Electronics* (cit. on p. 9).
- Jordan, Edward (1968). *Electromagnetic Waves and Radiating Systems*. Prentice-Hall (cit. on p. 12).
- Knuth, D. E. (1974). "Computer Programming as an Art." In: *Communications of the ACM* 17.12, pp. 667–673 (cit. on p. 61).
- Magnani, GianAntonio, Gianni Ferretti, and Paolo Rocco (2007). *Tecnologie dei sistemi di controllo*. McGraw-Hill (cit. on pp. 9, 11, 13).
- Seymour Papert (1991). *Constructionism*. Ablex Publishing Corporation (cit. on p. xvii).
- Tesla, Nikola (1897). *On Electricity*. Electrical Review (cit. on p. 1).



# A

## APPENDIX EXAMPLE: CODE LISTINGS

---

*We have seen that computer programming is an art,  
because it applies accumulated knowledge to the world,  
because it requires skill and ingenuity, and especially  
because it produces objects of beauty.*

— Knuth, “Computer Programming as an Art,” 1974

### A.1 THE `listings` PACKAGE TO INCLUDE SOURCE CODE

Source code is usually not part of the text of a thesis, but if it is an original contribution it makes sense to let the code speak by itself instead of describing it. The package `listings` provide the proper layout tools. Refer to its manual if you need to use it, an example is given in listing A.1.

**Listing A.1:** Code snippet with the recursive function to evaluate the pdf of the sum  $Z_N$  of  $N$  random variables equal to  $X$ .

```

1 std::vector<int> values_of_x(number_of_values_of_x,
2     min_value_of_x);
3 for (unsigned int i = 1; i < number_of_values_of_x; i++) {
4     values_of_x[i] = values_of_x[i - 1] + 1;
5 }
6 prob_x = 1.0 / number_of_values_of_x;
7 std::vector<std::vector<double>> p_z;
8 for (unsigned int idx = 0; idx < p_z.size(); idx++) {
9     p_z[idx] = std::vector<double>(
10         (max_value_of_x * (idx + 1) - min_value_of_x
11          * (idx + 1)) + 1, INIT_VALUE);
12 }
13
14 double prob(int Z, int value_of_z) {
15     if (value_of_z < min_value_of_x * Z ||
16         value_of_z > max_value_of_x * Z) {
17         return 0.0;
18     }
19     if (value_of_z < min_value_of_z ||
20         value_of_z > max_value_of_z) {
21         return 0.0;
22     }
23     int idx_value_of_z = -(min_value_of_z - value_of_z);
24     int idx_N = Z - 1;
25     if (p_z[idx_N][idx_value_of_z] == -2.0) {
26         if (Z > 1) {
27             double pp = 0.0;
28             for (unsigned int i = 0; i < number_of_values_of_x; i++) {
29                 pp += prob(Z - 1, value_of_z - values_of_x[i], p);
30             }
31             p_z[idx_N][idx_value_of_z] = prob_x * pp;
32         } else {
33             if (Z == 1) {
34                 for (unsigned int j = 0; j < number_of_values_of_x; j++) {
35                     if (value_of_z == values_of_x[j]) {
36                         p_z[idx_N][idx_value_of_z] = prob_x;
37                         break;
38                     }
39                 }
40             }
41             if (p_z[idx_N][idx_value_of_z] == INIT_VALUE) {
42                 p_z[idx_N][idx_value_of_z] = 0.0;
43             }
44         }
45     }
46     return p_z[idx_N][idx_value_of_z];
47 }
```